Studies of Structures, Quadratic Electro-Optic Effect and Rechargeable Battery Characteristics in Specific Nonconjugated Conductive Polymers including Trans-1,4-Polyisoprene

by

Sapana Shrivastava

A thesis submitted to the Graduate Faculty of
Auburn University
in partial fulfillment of the
requirements for the Degree of
Master of Science

Auburn, Alabama
May 9th, 2011

Keywords: Nonconjugated conductive polymer, Trans-polyisoprene, Quadratic electro-optic effect, X-ray structure, Rechargeable batteries, Thermal properties

Approved by

Mrinal Thakur, Chair, Professor of Mechanical Engineering
Dan Marghitu, Professor of Mechanical Engineering
Thomas Baginski, Professor of Electrical and computer Engineering

Abstract

The structures, quadratic electro-optic effect and rechargeable battery characteristics in specific nonconjugated conductive polymers have been studied. FTIR spectroscopy, x-ray diffraction, optical absorption, differential scanning calorimeter and optical microscopy have been used to study structures of nonconjugated conductive polymers including in particular, trans-1,4-polyisoprene. This is partly because trans-1,4-polyisoprene is semicrystalline in structure. Quadratic electro-optic effect has been measured at different wavelengths using field-induced birefringence method. Rechargeable batteries involving doped nonconjugated conductive polymer as an electrode were studied for enhanced efficiency.

The optical absorption spectrum of trans-1,4-polyisoprene at low doping of iodine shows two peaks: one at 4.2eV due to radical cation and the other at 3.2eV due to charge-transfer. Doping leads to a reduction of the intensity of =C-H bending vibration-band due to formation of radical cations upon charge-transfer. X-ray diffraction results showed the γ-phase crystal structure for undoped trans-polyisoprene. Upon iodine-doping intensities of specific diffraction peaks slightly increased but the d-spacings of all the peaks remained essentially unchanged. This indicates that the crystal structure remains essentially the same (γ-phase) except iodine atoms are deposited close to specific lattice planes.

Quadratic electro-optic measurements have been made using field-induced birefringence method at 633 nm and 1550 nm. A modulation depth of 0.15% has been observed at 1550 nm for an applied field of 1.15 V/μm for a 0.37μm thick film. The modulation depth had a quadratic

dependence on applied field. The Kerr coefficients as measured $3.5x10^{-10}$ m/V^2 at 633nm and $2.5x10^{-10}$ m/V^2 at 1550nm are exceptionally large and has been attributed to the subnanometer size metallic domains (quantum dots) formed upon doping and charge-transfer.

Thermal properties of the nonconjugated polymer trans-1,4-polyisoprene have been studied before and after doping with iodine using a differential scanning calorimeter (DSC) over the temperature range of -50 ◦C to 110◦C. The T_m of undoped trans-1,4-polyisoprene has been found to be at 60 ◦C. After doping the Tm transition was not clearly observable.

Rechargeable batteries have been constructed with sodium chloride (NaCl) dissolved in water with polyvinyl alcohol as additive used as electrolyte, along with two electrodes: 1) stainless steel strip and 2) nonconjugated conductive polymer, iodine doped cis-polyisoprene (natural rubber). The batteries have been characterized measuring currents and voltages with many cycles of charging and discharging. A voltage of 1.5 volts and a maximum current of have been measured. Discharge rate of current has been recorded at definite intervals of time. Polyvinyl alcohol (PVA) has been added to electrolyte solution at 10-50 % weight of NaCl. Gradual slow down in discharge rate – significant increase in capacity has been observed with increase in concentration of PVA in the electrolyte solution.

Acknowledgments

I would like to take this opportunity to convey my gratitude to my academic advisor, Dr. Mrinal Thakur for his continued support throughout my research program at Auburn University, Auburn, AL. I would like to thank Dr. Dan Marghitu and Dr. Thomas Bagniski for serving on my advisory committee.

I appreciate all the help from my colleagues in Photonic Materials Research Laboratory, Ananthakrishnan Narayanan, Gurudutt Telang. I am thankful to all the people who helped directly or indirectly with my research. I am very grateful to my parents for all their support and encouragement. I am thankful to all my friends for their support

Table of Contents

List of Figures

List of Tables

CHAPTER 1

INTRODUCTION

The science and technology that deal with applications of light (photons) is known as Photonics. It has a wide range of applications involving emission, transmission, modulation, signal processing, switching etc. using light. It also associated with other fields i.e., medical science, material science, optics, electronics etc. Studies of linear and nonlinear optical properties of materials are at the heart of such applications in photonics. Novel nanomaterials and structures provide many new avenues for photonics applications. The present thesis includes investigations of such new materials that form organic nanometallic-like structures leading to exceptional nonlinear optical properties

In this fast-growing world, the demand for energy is increasing at very high rate, whereas energy sources are depleting at a much higher rate. Scientists and researchers are actively pursuing new sources of energy with natural resources i.e., wind energy, hydraulic energy, and, foremost solar energy (or light). Solar cells or photovoltaic cells are used as fuel, which convert light energy into electrical energy. There are some inorganic and organic materials, which absorb light from the source, release electrons and produce electricity.

Inorganic materials have been the main ingredient of photovoltaic cell for a few decades, but its fabrication and installation is costly. To conquer these drawbacks of inorganic materials, organic material got the attention of photonic researchers and engineers. Because of their low

dielectric property and high optical property, they are not only used in photovoltaic cell, they are also used in many other application of photonics, i.e., electro-optics, absorption etc.

Today we are dependent on many small and large devices, which operate on batteries. Inorganic materials are widely used as electrodes for rechargeable batteries, but life and performance are not adequate. To get overcome these problems and limitations, various researchers and scientists are trying to invent new techniques and resources. Nonconjugated conductive polymers are a great discovery in the photonics, electronic and telecommunication fields. To validate this fact, more evident is provided by our research, which is divided into the following fields:

1. Thermal properties of nonconjugated conductive polymers (Trans-1,4-polyisoprene, Poly(β-pinene), Cis-polyisoprene) by using Differential Scanning Calorimeter, before and after doping with iodine.
2. Quadratic electro-optics effect and other multi order nonlinearities of nonconjugated conductive polymer, Trans-1,4-polyisoprene doped with iodine at shorter wavelength
3. Rechargeable batteries and photovoltaic cell with nonconjugated conductive polymers.

These works are systemically organized in different chapters. The overall goals of this research and studies are discussed in chapter 2, titled as Objective. The basic theories and concepts of photonic and nonlinear optics, that support this thesis, are briefly discussed as Background in Chapter 3. The physical and electrical properties of nonconjugated conductive polymers have been discussed in chapter 4.

Chapter 5 gives brief a idea about rechargeable batteries, and it demonstrates each step of making new rechargeable batteries based on nonconjugated conductive polymer trans-1,4-polyisoprene. Trans-1,4-polyisoprene have been studied by various spectroscopic methods and

tested for electro-optics effect, explained in chapter 6. Optical nonlinear properties of various nanomaterials and metal nanoparticles are explained and compared with optical properties of nonconjugated conductive polymer trans-polyisoprene, in chapter 7.

Two unfinished works (collaborative); the first one is, study of thermal properties of nonconjugated polymer by using differential scanning calorimeter; the second is, reflectivity and absorption coefficient have been calculated on MATLAB software, discussed in chapter 8. The whole research has been summarized in chapter 9

CHAPTER 2

OBJECTIVES

The overall objective of this research project is to study structures, quadratic electro-optic effect, and rechargeable battery characteristics of specific nonconjugated conductive polymers including trans-1,4-polyisoprene. The structures will be studied using FTIR, x-ray diffraction, optical absorption, differential scanning calorimetry and optical microscopy. Trans-polyisoprene being semicrystalline, x-ray diffraction will be used to study any crystal structural change upon doping with iodine. FTIR, optical absorption, optical microscopy, and differential scanning calorimetry will be used to look into the chemical and other structural changes of the polymer.

The quadratic electro-optic effect in the polymer will be studied using field-induced birefringence technique, and the Kerr coefficients will be determined. The measurements will be made at 633 nm and 1550 nm following established procedure. The modulation depths for different applied ac fields will be measured using photodiodes along with oscilloscope and lock-in amplifier. The measured optical nonlinearities will be correlated to the nanometallic-like structures of doped polymers.

Potentially low-cost rechargeable batteries will be fabricated using specific doped nonconjugated conductive polymers as one of the electrodes and with lower cost counter electrodes and electrolytes. The batteries will be characterized for rechargeability and capacity. The polymers will include cis-polyisoprene (natural rubber). The polymer films will be doped with iodine before use as the electrodes.

Overall, this project will elucidate structures, electro-optics, and rechargeable battery characteristics in specific doped nonconjugated conductive polymers.

CHAPTER 3

BACKGROUND

Nonlinear optics represents one of the most recent advancements in Photonics. It deals with interaction of laser light with materials under high optical intensity or with an applied electric field. Optical nonlinearity occurs when a material system gives a nonlinear response with applied fields. The effects may include: frequency conversion, linear and quadratic electro-optic modulation/switching, all-optical modulation, optical limiting and others.

3.1 Governing Maxwell's Equation

The propagation of light is governed by few fundamental equations known as Maxwell's equations. Light is an electromagnetic wave for which the direction of propagation and the electric and magnetic fields are mutually perpendicular to each other. The Maxwell's equations for electric and magnetic field vectors $\vec{E}$ and $\vec{H}$, and $\vec{B}$ and $\vec{D}$ electric and magnetic displacement vectors, have the following differential forms. [9, 10]

$$\nabla.\overrightarrow{\mathrm{D}} = \rho \qquad \text{Eqn. (3.1)}$$

$$\nabla.\overrightarrow{\mathrm{B}} = 0 \qquad \text{Eqn. (3.2)}$$

$$\nabla \times \overrightarrow{E} = -\frac{\partial \overrightarrow{\mathrm{B}}}{\partial \mathrm{t}} \qquad \text{Eqn. (3.3)}$$

$$\nabla \times \overrightarrow{\mathrm{H}} = \mathrm{J} + \frac{\partial \overrightarrow{\mathrm{D}}}{\partial \mathrm{t}} \qquad \text{Eqn. (3.4)}$$

ρ and *J* are electric charge and current densities. With dielectrics media, there is no free charge and no current flow, therefore ρ and *J* are zero.

Distortion of atomic orbital's have been descried by polarization magnetization, caused by electromagnetic field. Conductivity is defined by tbhe flow of electric charges. The following relations hold. [5, 8-10]

$$\vec{B} = \mu_0(\vec{H} + \vec{M}) \qquad Eqn.(3.5)$$

$$\vec{J} = \sigma\vec{E} \qquad Eqn(3.6)$$

$$\vec{P} = \varepsilon_0\chi\vec{E} \qquad Eqn(3.7)$$

$$\vec{D} = \varepsilon_0\vec{E} + \vec{P} \qquad Eqn(3.8)$$

$$\vec{D} = \varepsilon_0(1+\chi)\vec{E} \qquad Eqn(3.9)$$

where ε_0 = vacuum permittivity (dielectric constant)

μ_0 = Vacuum permeability

P = Induced polarization due to applied electric filed

M = Induced magnetization due to applied magnetic field.

3.2 Wave Equation

The propagation of electromagnetic waves in a medium or in a vacuum has been described by partial differential equations. They are written as:

$$\nabla\times\nabla\times\vec{E} = \nabla\times(-\frac{\partial\vec{B}}{\partial t}) \qquad Eqn(3.10)$$

The final wave equation derived as:

$$\nabla\times\nabla\times\vec{E} + \frac{1}{c^2}\frac{d^2E}{dt^2} = -\mu_0\frac{d^2P}{dt^2} - \mu_0\frac{dJ}{dt} \qquad Eqn.(3.11)$$

3.3 Linear and Nonlinear Optical Properties

Optical materials can be classified into two categories

1. Materials with predominantly linear optical properties
2. Materials with second, third or higher order optical nonlinearities

In an isotropic dielectric media; polarization occur due to applied electric field, while in anisotropic media it may not be. The electric field and linear polarization are expressed as

$$\overrightarrow{\mathrm{E}}\,(\vec{r}\,,\mathrm{t}) = \overrightarrow{\mathrm{E}}_{\,0}\exp\left(\overrightarrow{k}\,.\vec{r} - \omega.t\right) + c.c \qquad Eqn.(3.12)$$

$$\vec{P} = \varepsilon_0\chi^{(1)}\overrightarrow{\mathrm{E}} \qquad Eqn.(3.13)$$

And the real dielectric constant is expressed as

$$\varepsilon = 1 + \chi^{(1)} = \{n + i\alpha\frac{c}{2\omega}\}^2 \qquad Eqn.(3.14)$$

n is refractive index, α is absorption coefficient and $\chi^{(1)}$ is linear susceptibilities. Nonlinear optical media, the propagation of light is not so simple. The polarization depends on higher powers on electric field and is usually highly anisotropic.

$$\vec{P} = \varepsilon_0(\chi^{(1)}\vec{E}(t) + \chi^{(2)}\vec{E}^2(t) + \chi^{(3)}\vec{E}^3(t) + \chi^{(4)}\vec{E}^4(t) + \cdots) \qquad (3.15)$$

$$\vec{P} = \vec{P}^{(1)}(t) + \vec{P}^{(2)}(t) + \vec{P}^{(3)}(t) + \cdots \qquad (3.16)$$

Where $\chi^{(2)}$ and $\chi^{(3)}$ are second and third order susceptibilities, after truncating linear part of series, $\vec{P}^{(1)}(t) = \chi^{(1)}\vec{E}(t)$, the rest of the series is known as nonlinear polarization.

$$\overrightarrow{P_{NL}} = \varepsilon_0(\chi^{(2)}\vec{E}^2(t) + \chi^{(3)}\vec{E}^3(t) + \chi^{(4)}\vec{E}^4(t) + \cdots) \qquad (3.17)$$

3.4 Nonlinear Optical processes

There are various outcomes when photons interacted with a nonlinear optical medium. These are as follows.

1. Sum frequency generation, Second harmonic generation
2. Difference frequency generation
3. Third harmonic generation
4. Optical rectification
5. Linear electro-optic effect

6. Quadratic Electro-optic effect

These depend on experimental, or device configuration and the effect is larger for materials with higher nonlinearities.

3.4.1 Sum-Frequency Generation

When a strong applied field, frequency ω_1 and a weak applied field frequency ω_2 interact with nonlinear material, there is a situation in which the strong signal ω_1, merge with the weak signal ω_2 and produced higher frequency signal ω_3.

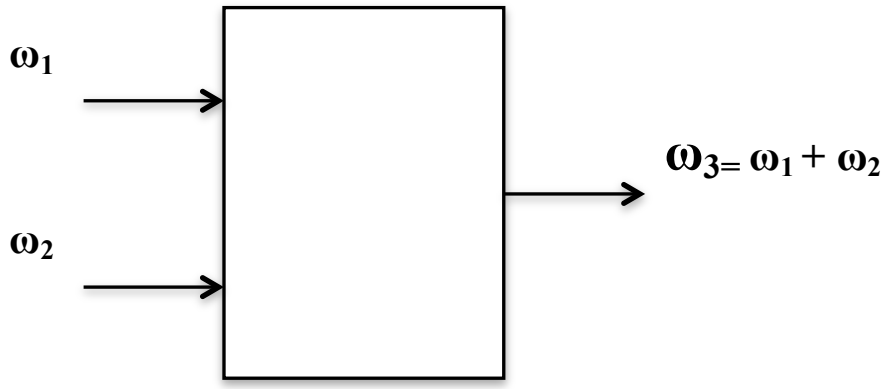

Figure 3.1: Sum-Frequency Generation

3.4.2 Difference-Frequency Generation

This process is similar to sum of frequency. In this processes, applied input fields (with frequencies ω_1 or ω_2 and ω_3) interact with lossless nonlinear material to produce an output signal at difference frequency $(\omega_2 = \omega_3 - \omega_1)$ or $(\omega_1 = \omega_3 - \omega_2)$. Shown in Figure 3.2

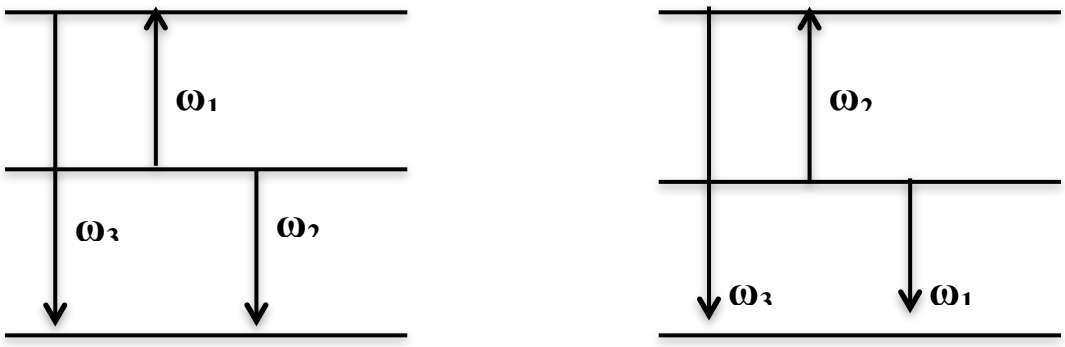

Figure 3.2: Difference of Frequency Generation

3.4.3 Second harmonic Generation

In this nonlinear process, full permutation symmetry of susceptibilities have been seen, which are cause by two fundamental frequencies, ω_1 and $\omega_2 = 2\omega_1$ second harmonic frequency as in Figure 3.3

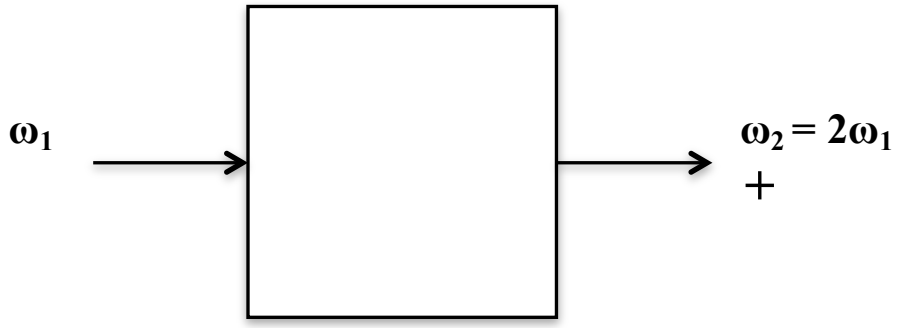

Figure 3.3: Second Harmonic Generation

3.4.4 Third Harmonic Generation

This is also known as optical frequency multiplier. It is also similar second harmonic generation and produced higher frequency and shorter wavelength than second harmonic generation. It is widely used in high power lasers and Inertial Confinement Fusion experiments

3.4.5 Optical Rectification

Nonlinear second order susceptibility is the main cause of nonlinear optical processes, i.e. sum of frequency and difference of frequency. There is a different case with two equal frequencies, in second order susceptibility given as in Eqn.()

$$\chi_{kij}^{(2)}(0,\omega,-\omega) = \chi_{jki}^{(2)}(0,\omega,\omega)$$

The real part of $\chi_{jki}^{(2)}(0,\omega,\omega)$ defines Pockels effect or linear electro-optics, and describes change in refractive index due to applied electric field, whereas the real part of $\chi_{kij}^{(2)}(0,\omega,-\omega)$ define an other process known as optical rectification. It originate due to quasi – DC generation optical nonlinear medium

3.5 Phase Matching Consideration

When two frequencies are mixing in such a way, they produce sum-frequency generation without change in intensity of input beams; frequency of output beam is given by $\omega_3 = \omega_1 + \omega_2$. Relationship between wave number 'k', refractive 'n' index and frequency 'ω' is shown below

$$k_j = \frac{n_j \omega_j}{\mathrm{c}} \qquad Eqn(3.18)$$

where 'c' = velocity of light.

So according to sum of frequencies, condition for phase matching is given by

$$\Delta k = k_1 + k_2 - k_3 \qquad Eqn(3.19)$$

Output intensity is $I_3 = I_3(max)\frac{sin^2(\Delta kL/2)}{(\Delta kL/2)^2}$. The condition for perfect phase match $\Delta k = 0$, which is difficult to achieve

3.6 Nonlinear optical properties

Optical materials behave nonlinearly when dealing with high optical frequency. These properties define ways that light propagates into the materials and they are very important in photonic field applications and ultrafast telecommunication devices. Nonlinear properties such as high refractive index and high optical absorption of material are very useful in laser surgeries and other medical equipment. There are some nonlinear properties explained below:

3.6.1 Nonlinear susceptibilities

Polarization induces in optical material due to alignment of dipoles in the same direction of the applied electrical field. Higher order polarization and susceptibilities have been studied for decades. Mainly second and third order susceptibility has been reported [8-10, 15]. Two electric $E_j(\omega_2)$ and $E_k(\omega_2)$ field interact with nonlinear materials, inducing second order nonlinear polarization

$$\overrightarrow{P_{\omega_3}} = 2\varepsilon_0 \Sigma \chi^{(2)}_{ijk}(\omega_3; \omega_3, \omega_3) E_j(\omega_1).E_k(\omega_2) \qquad Eqn.(3.20)$$

$$\overrightarrow{P_{\omega_3}} = 2\varepsilon_0 \Sigma d^{(2)}_{ijk}(\omega_3; \omega_1, \omega_2) E_j(\omega_1).E_k(\omega_2) \qquad Eqn.(3.21)$$

Where $\chi^{(2)}_{ijk}$ = Second order susceptibilities tensor

$d^{(2)}_{ijk}$ = Displacement induced due to change in electric field.

Second order susceptibility $\chi^{(2)}_{ijk}$,is absent in the centrosymmetric materials due to its inversion center

$$\chi^{(2)}\vec{E}^2(t) = -\chi^{(2)}\vec{E}^2(t) \qquad Eqn.(3.22)$$

Non-centrosymmetric has abilities for both second and third order susceptibilities. Third order susceptibility has been seen in third harmonic generation and χ^3_{ijk} is responsible for the Kerr effect, which cause nonlinear enhancement of refractive index of material, self and cross phase modulation [9-10,14].

Nonlinear properties of materials are represented as tensor χ_{ijk}, d_{ijk} or r_{ijk}, where *i, j and k* are dummy indices. General second order polarization expressed as

$$\vec{P}(\omega_n + \omega_m) = \sum_{jk}\sum_{nm} \chi^{(2)}_{ijk}(\omega_n + \omega_m; \omega_n, \omega_m)E_j(\omega_n).E_k(\omega_m) \qquad Eqn.(3.23)$$

from this expression we get different combination *of n,m,i , j and k.* These dummy indices are interchangeable

$$\chi^{(2)}_{ijk}(\omega_3 = \omega_1+\omega_2) = \chi^{(2)}_{jki}(\omega_1 = -\omega_2+\omega_3) \qquad Eqn(3.24)a$$

$$\chi^{(2)}_{kij}(\omega_3 = \omega_1+\omega_2) = \chi^{(2)}_{jki}(\omega_2 = \omega_3-\omega_1) \qquad Eqn(3.24)b$$

as long as indices are interchangeable, frequency argument can be changed and susceptibilities are equal and real in lossless medium. This process is known as intrinsic permutation symmetry of susceptibilities.[8-10]

3.6.2 Nonlinear Dielectric coefficient and Refractive index

Dielectric constant, absorption coefficient and refractive index are the function frequency or wavelength. Refractive index 'n' can be derived from a relationship between relative permittivity 'ε' or dielectric constant and relative permeability 'μ', seen in Eqn.(3.25)

$$n^2 = \varepsilon\mu \qquad Eqn.(3.25)$$

Usually at higher optical frequency, relative permeability of optical material become near unity.

From Eqn. (3.14) and Eqn (3.28)

$$n = \sqrt{1+\chi} \qquad Eqn.(3.26)$$

The dependency of refractive index of material on optical frequency is known as *Chromatic depression.* According to various literature reviews, refractive index for glasses and crystals, seen in range of 1.4 – 2.8, lie in visible spectra region [72].

Generally, semiconductors also show good nonlinear properties, i.e. higher refractive indices with strong absorption. A very good example is Gallium Arsenide (GaAs) with refractive index of ~3.5 at 1μm, due to strong absorption at different wavelengths below the band gap wavelength of ~870nm [72] It has also been seen that refractive index increase towards shorter wavelength; as can be seen for fused silica in Figure 3.4.

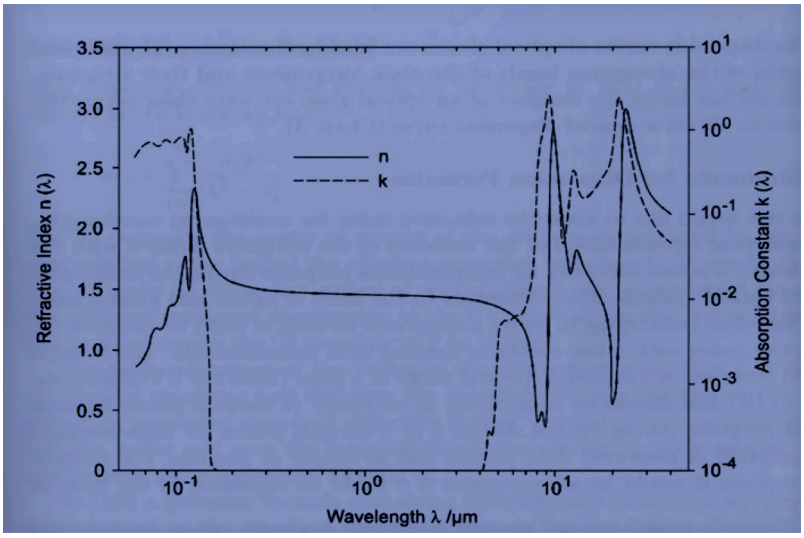

Figure 3.4: Refractive index and Absorption coefficient of fused silica (SiO_2 Glass) [70]

Nonlinear properties are complex number, have a real part and an imaginary part and both play very important roles in optical sciences. Like susceptibility, refractive index and dielectric constant, they all can be represented as complex numbers, as shown in Eqns.(3.27)

$$\chi(\omega) = \chi'(\omega) + i\chi''(\omega) \qquad Eqn(3.27)a$$

$$\varepsilon(\omega) = \varepsilon'(\omega) + i\varepsilon''(\omega) \qquad Eqn(3.27)b$$

$$\eta(\omega) = n(\omega) + ik(\omega) = \sqrt{1 + \chi'(\omega) + i\chi''(\omega)} \qquad Eqn(3.27)c$$

where $\chi'(\omega)$, $\varepsilon'(\omega)$ and $n(\omega)$ are real parts and $\chi''(\omega)$, $\varepsilon''(\omega)$ and $k(\omega)$ are imaginary parts of susceptibility, dielectric constant and refractive index respectively.

As per the theory of analytic complex numbers, relationships have been deduced, which relates the real part and imaginary part through an integral function. The great researchers, **Ralph Kronig** and **Hendrik Anthony Kramers** found relations between the real part and the imaginary part of optical properties of materials, as given below [10, 68-70]. Relation between

real and imaginary parts of the dielectric constant and susceptibility are given below in Eqn. (3.31) and Eqn. (3.32)

$$\varepsilon'(\omega) = 1 + \frac{2}{\pi}\int_{0}^{+\infty} \frac{\omega'\,\varepsilon''(\omega')}{\omega'^2 - \omega^2}\,d\omega' \qquad Eqn(3.28)$$

$$\chi'(\omega) = \frac{2}{\pi}\int_{0}^{+\infty} \frac{\omega'\,\chi''(\omega')}{\omega'^2 - \omega^2}\,d\omega' \qquad Eqn(3.29)$$

Refractive index expressed in term of absorption coefficient as in Eqn. (3.30)

$$n(\omega) = 1 + \frac{c}{\pi}\int_{0}^{+\infty} \frac{\alpha(\omega')}{\omega'^2 - \omega^2}\,d\omega' \qquad Eqn(3.30)$$

Phase shift expressed in term of reflectivity as in Eqn. (3.31)

$$\varphi(\omega) = 1 + \frac{2}{\pi}\int_{0}^{+\infty} \frac{\ln\{R(\omega')/R(\omega)}{\omega'^2 - \omega^2}\,d\omega' \qquad Eqn(3.31)$$

These equations are known as *Kramers-Kronig relations,* and used for correction in refractive index and reflectivity (caused by some excitation in media) due to change in absorption coefficien

3.7 X-ray Crystallography

In 1912, Max Von Laue suggested that x-rays have shorter wavelengths of about 1Å which is comparable to lattice spacings in crystals, therefore, x-rays could be used for diffraction to study internal structures of crystals. This method of studies is called x-ray crystallography [24]. This is widely used for finding the arrangement of atoms in crystals. Basically, x-rays of a fixed wavelength impinging on a material, diffract at specific directions with certain angles. The

pattern of diffracted maxima is recorded along with intensities. Diffractometer scans show peaks with different intensities verses angles or d-spacings. From such data, atomic and/or molecular arrangements within crystals can be determined with high precision [23, 25-29].

3.7.1 Type of crystals

Crystal structure has been classified in six basic crystal systems according to their axes of a unit cell and angles between axes. They are named on the basis of their orientation and number of sides of a unit cell, which can be seen in Table 3.1

Table 3.1: crystal structures with their axes, angles and orientations [30-32]

Crystal system (α, β, γ)	Crystal axes and angles	Orientation of axes
Triclinic	$a \neq b \neq c$, $\alpha \neq \beta \neq \gamma$	Unspecified
Monoclinic	$a \neq b \neq c$, $\alpha = \beta = 90^0 \neq \gamma$	c parallel to 2
Orthorhombic	$a \neq b \neq c$, $\alpha = \beta = \gamma = 90^0$	a, b and c, must parallel to 2's
Tetragonal	$a_1 = a_2 \neq c$, $\alpha = \beta = \gamma = 90^0$	c parallel to 4
Cubic (isometric)	$a_1 = a_2 = a_3$, $\alpha = \beta = \gamma = 90^0$	a_1, a_2 and a_3, must parallel to 4's
Hexagonal	$a_1 = a_2 \neq c$, $\alpha = \beta = 90^0$, $\gamma = 120^0$	c parallel to 6 (or 3)

Where 'a' , 'b' , 'c' are axes and α ,β ,γ are angle between axes of unit cell. Crystallographers found a *law of rotational indices* , intercepts made by any plane on axes, denoted by *a/h, b/k and c/l.* where h, k, and l are nonzero value, widely accepted as **Miller Indices** introduce by W.H. Miller [30] They are written as (h,k,l) and represent all parallel planes. Miller indices can be for

2-D and 3-D. For example, a cubic lattice has planes, which are represented in term of miller indices (100), (010), (001) and (111).

3.7.2 Bragg's Law

The relationship between d-spacing, angle of diffraction and wavelength of X-ray has been developed by two Physicists, William Henry Bragg (father) and William Lawrence Bragg (son) in 1912. They shared the Nobel prize in 1915. The light waves with wavelength λ strike various crystal planes and reflect at different scattering angles, which are equal to the incident angle, demonstrated by Figure 3.5

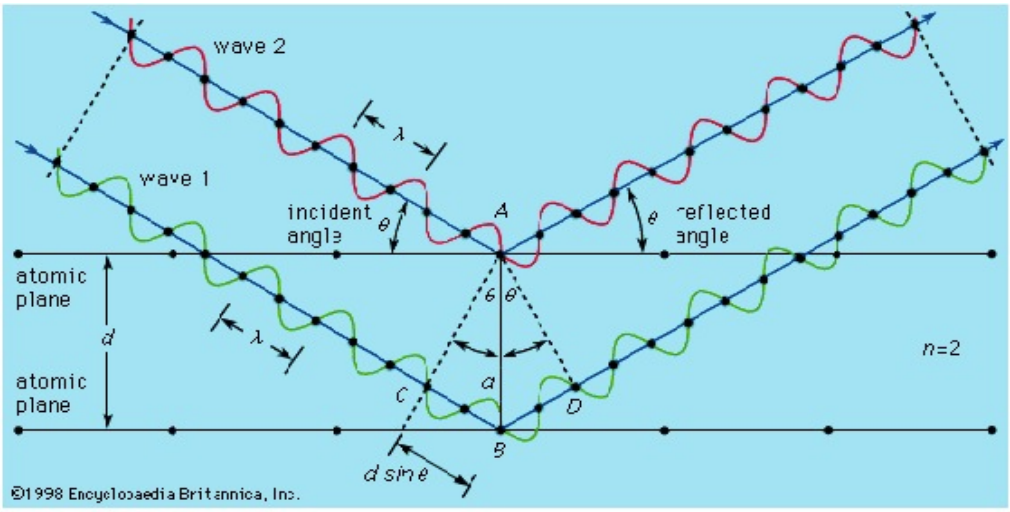

Figure 3.5: Bragg's Law [22]

The equation found by Braggs, which relates wavelength of light, angle of reflection and distance between two atomic planes is given in Eqn. (3.32)

$$2d_{hkl}sin\theta = \lambda \qquad Eqn(3.32)$$

where λ = wavelength

θ = angle of diffraction

d_{hkl} = interplanar spacing for (hkl) planes

'The relationship between d_{hkl} with unit cell parameter (a) of a cubic crystal is given by

$$d(hkl) = \frac{a}{\sqrt{h^2 + k^2 + l^2}} \qquad Eqn(3.33)$$

For example, X-ray diffraction of NaCl has been shown in Figure 3.6. X-ray waves diffract at different angles with different intensities and show peaks on the x-ray pattern. Each peak represented by unique miller indices, which gives an idea about the plane from which waves are reflecting. In NaCl X-ray diffraction graph, the 3rd peak at angle 23 degrees (approx.) has miller Indices (220). D-spacing of the plane (220) can be calculated from the Eqn.(3.33), which is equal to 1.9707Å

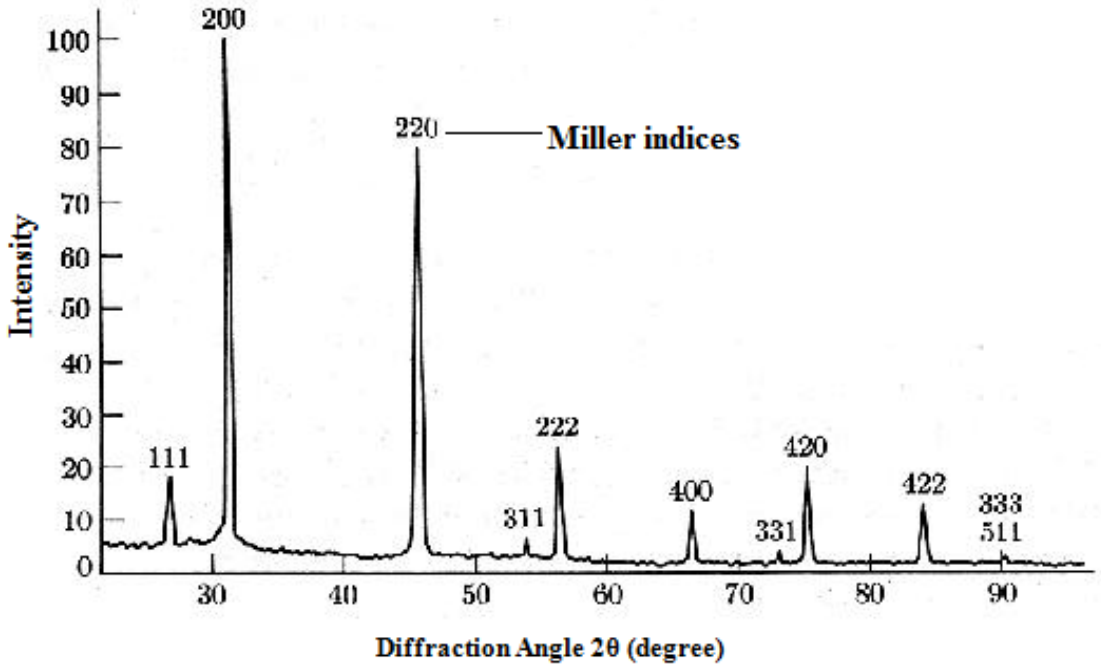

Figure 3.6: X-ray diffraction of NaCl [33]

3.8 FTIR Spectroscopy

Absorption, transmission and emission of light at different wavelengths are three specific keys to characterize any material. Infrared spectroscopic methods are used to identify various functional groups (i.e. ketone, ester, acid etc.) by obtaining absorption or emission spectra. Fourier transforms spectroscopy is used for identification and quantitative determination of different functional groups in polymers and other organic compound. It gives peaks at different wavelengths depending on the vibrational energies of the chemical groups. Thus, each peak corresponds to a specific chemical group

Molecules consist of atoms with different bond lengths and bond angles. Either stretching or bending vibration may have resonances at specific infrared wavelengths. Different stretching and bending wavelengths or wave-numbers are expected for groups such as CH_2, CO, CH and NH groups. The total transmission 'T' can be recorded as

$$T = \frac{I}{I_o} = e^{c\varepsilon l} \qquad Eqn.(3.34)$$

and actual IR absorption 'A'can be calculated by the Beer Lambert Law

$$A = -ln(T) = e^{c\varepsilon l} \qquad Eqn(3.35)$$

For examples, organic acids have O-H group, which absorbs strongly at ~ 3300-2500cm^{-1} and C-O absorbs near 1100-1300cm^{-1}. Ketone have strong absorption due to the presence of C=O carbonyl group near 1725-1705cm^{-1} [73,74] Similarly, these organic functional group have different absorption bands in different class of materials, i.e. ester, aldehyde etc.

3.9 Electro-Optic Effect

The electro-optic effect can be rationalized by change in refractive index, occuring due to applied electric field. If change is linear to the applied field, it gives linear electro optic effect or Pockels effect, described in term second order susceptibility.

$$\overrightarrow{P_{\omega_3}} = 2\varepsilon_0 \Sigma \chi^{(2)}_{ijk}(\omega_3; \omega_3, \omega_3) E_j(\omega_1).E_k(\omega_2) \qquad Eqn(3.36)$$

Displacement vector, as defined earlier, is also given by

$$D_i = \sum_j \varepsilon_{ij} E_j \qquad Eqn(3.37)$$

and in matrix form

$$\begin{bmatrix} D_x \\ D_y \\ D_z \end{bmatrix} = \begin{bmatrix} \varepsilon_{xx} & \varepsilon_{xy} & \varepsilon_{xz} \\ \varepsilon_{yx} & \varepsilon_{yy} & \varepsilon_{yz} \\ \varepsilon_{zx} & \varepsilon_{zy} & \varepsilon_{zz} \end{bmatrix} \begin{bmatrix} E_x \\ E_y \\ E_z \end{bmatrix} \qquad Eqn(3.38)$$

dielectric permeability tensor is symmetric matrix, so $\varepsilon_{ij} = \varepsilon_{ji}$, it can be reduced into a diagonal matrix by transformation method, as demonstrated in Eqn.(3.37), which defines a new coordinate system, called Principle Axis System

$$\begin{bmatrix} D_x \\ D_y \\ D_z \end{bmatrix} = \begin{bmatrix} \varepsilon_{XX} & 0 & 0 \\ 0 & \varepsilon_{YY} & 0 \\ 0 & 0 & \varepsilon_{ZZ} \end{bmatrix} \begin{bmatrix} E_x \\ E_y \\ E_z \end{bmatrix} \qquad Eqn(3.39)$$

In an anisotropic material, energy density of wave propagation is given by

$$U = \frac{1}{8\pi} D.E = \frac{1}{8\pi} \sum_{ij} \varepsilon_{ij} E_i E_j \qquad Eqn(3.40)$$

and principal axis system energy density is defined as

$$U = \frac{1}{8\pi}\left[\frac{D_X^2}{\varepsilon_{XX}} + \frac{D_Y^2}{\varepsilon_{YY}} + \frac{D_X^2}{\varepsilon_{ZZ}}\right] \qquad Eqn(3.41)$$

it can be rewritten as

$$\frac{X^2}{\varepsilon_{XX}} + \frac{Y^2}{\varepsilon_{YY}} + \frac{Z^2}{\varepsilon_{ZZ}} = 1 \qquad Eqn(3.42)$$

where $X = \left(\frac{1}{8\pi U}\right)^{1/2} . D_x$, $Y = \left(\frac{1}{8\pi U}\right)^{1/2} . D_y$ and $Z = \left(\frac{1}{8\pi U}\right)^{1/2} . D_z$

There is relation between refractive index 'n' and dielectric permeability 'ε', $n = \sqrt{\varepsilon}$, so Eqn. (2.29) can be rewritten in terms of refractive index for principal axis coordinate system as

$$\left(\frac{1}{n^2}\right)_1 x^2 + \left(\frac{1}{n^2}\right)_2 y^2 + \left(\frac{1}{n^2}\right)_3 z^2 = 1 \qquad Eqn(3.43)$$

this equation know as optical indicatrix or index ellipsoid [8-10, 16]. But the general form of ellipsoid equation is expressed as

$$\left(\frac{1}{n^2}\right)_1 x^2 + \left(\frac{1}{n^2}\right)_2 y^2 + \left(\frac{1}{n^2}\right)_3 z^2 + \left(\frac{1}{n^2}\right)_4 yz + \left(\frac{1}{n^2}\right)_5 xz + \left(\frac{1}{n^2}\right)_6 xy = 1 \qquad Eqn(3.44)$$

There is a modification has done for low frequency electric field, known as impermeability tensor η_{ij} which is defined as

$$E_i = \sum_j \eta_{ij} D_j \qquad Eqn(3.45)$$

Now, Eqn. (3.47) can be modifid as

$$\eta_{11}\, x^2 + \eta_{22} y^2 + \eta_{33}\, z^2 + \eta_{23} yz + \eta_{13}\, xz + \eta_{12}\, xy = 1 \qquad Eqn(3.46)$$

This equation can be explained by a power series with applied electric field as

$$\eta_{ij} = \eta_{ij}^{(0)} + \sum_{k} r_{ijk}\, E_k + \sum_{kl} s_{ijk}\, E_k\, E_l + \ldots\ldots \qquad Eqn(3.47)$$

Where r_{ijk} = known a coefficient of Linear electro-optic effect

s_{ijk} = known as coefficient of quadratic electro-optic effect

CHAPTER 4

NONCONJUGATED CONDUCTIVE POLYMERS

Organic polymers and inorganic materials are widely used in electronics and telecommunication. Conjugated polymers are well known to be electrically conductive with various applications. In 1988, Thakur first reported that nonconjugated polymers with at least one double bond in the repeat unit can be electrically conductive upon doping, similar to conjugated polymers.

Various nonconjugated conductive polymers, including poly(β-pinene) (PBP), cis-polyisoprene (CPI) and trans-1,4-polyisoprene (TPI), have been studied. Conductivity of nonconjugated polymers has been studied in the past for doping with different dopants i.e. iodine, $SnCl_4$ and $SbCl_5$. The conductivity of nonconjugated polymer is based on number fraction of double bonds, which is the ratio of double bonds to the total number of bonds along the polymer chain. Conductivity increases rapidly with the increase in the number fraction of double bonds. Conjugated polymers have double bonds alternating with single bonds; their number fraction of double bonds is 1/2, while nonconjugated conductive polymers have double bond number fractions less than ½. [1,2,4,12]

4.1 Poly (β-pinene) (PBP)

PBP has been reported as a novel nonconjugated conductive polymer. It has a ring type structure, in which double bond repeated after every sixth carbon; therefore it has 1/6 number fraction of double bonds and its conductivity increases rapidly upon doping with iodine.

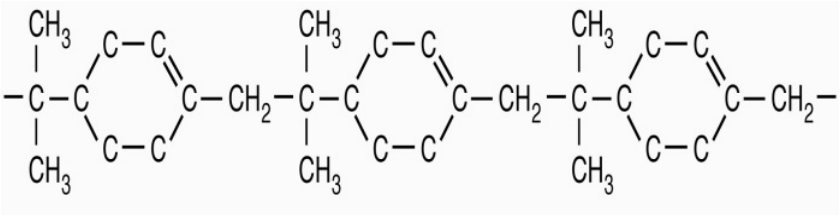

Figure 4.1: Molecular structure of Poly(β-pinene)

Conductivity of PBP has been measured before and after doping with iodine, it increased by many order of magnitude upon doping with iodine, 0.008 S/cm, due to formation of radical-cation and charge transfer from double bond to dopant. It shows large nonlinear properties and has large Kerr coefficient, 1.6×10^{-10} m/V^2 at 1550 nm [75,78]

4.2 Polyisoprene

Polyisoprene has two conformations: cis-1,4-polyisoprene and trans-1,4-polyisoprene. Both have the same molecular formula and different orientations of the carbon atoms in the structures. In both, every fourth carbon has double bond; number fraction of double bond is ¼ and their conductivity also increases by many orders of magnitude after doping with iodine. They have maximum conductivity of ~ 0.1 S/cm. [2,12]

4.2.1 Cis-polyisoprene (CPI):

The molecular structure of cis-1,4-polyisoprene (natural rubber) is shown in Fig.4.4. It is an amorphous polymer; give smooth film, when deposited on glass slide by various methods.

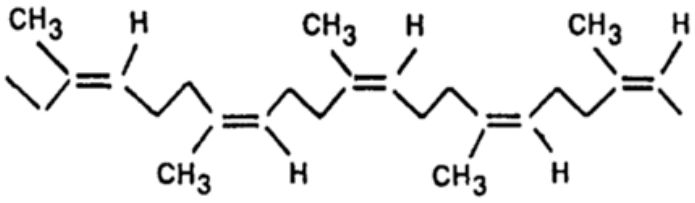

Figure 4.2: Molecular structure of Cis-polyisoprene

Absorption spectra of cis-polyisoprene before and after iodine-doping are shown in Figure 4.3. Kerr coefficient for Cis-polyisoprene has already been reported, which is $1.6x10^{-10}$ m/V^2 and higher than Poly (β-pinene) [12].

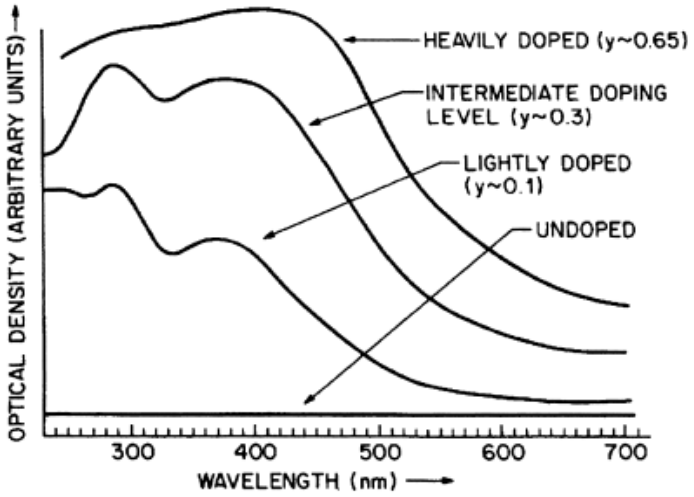

Figure 4.3: Absorption Spectra of CPI at different doping level with iodine

4.2.2 Trans-1,4-polyisoprene (TPI):

It is a polycrystalline material with a planar zig-zag molecular structure. Characterization had been done of TPI by the study of its thin film with optical absorption, FTIR, X-ray diffraction and other spectroscopic methods.

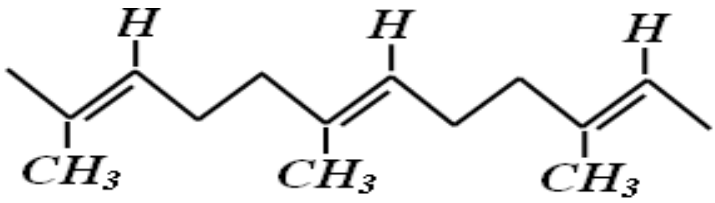

Figure 4.4: Molecular structure of Trans-1,4- polyisoprene [1]

Trans-1,4-polyisoprene study shows that it is a polycrystalline, shown in Figure 7.It has been recently known for its conductivity upon doping with iodine.

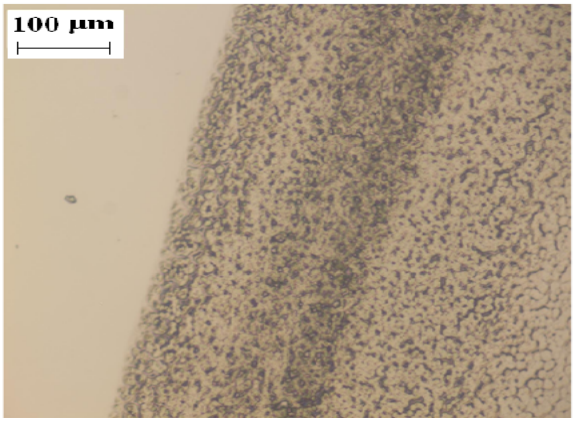

Figure 4.5: Micrograph of trans-polyisoprene film

This research work has been undertaken to study structures of iodine doped Nonconjugated conductive polymers, Cis-polyisoprene and Trans-polyisoprene, and their large nonlinear optical properties.

CHAPTER 5

NONCONJUGATED CONDUCTIVE POLYMER, DOPED CIS-POLYISOPRENE, AS ELECTRODE IN RECHARGEABLE BATTERIES

5.1 Introduction

Batteries have a great importance in electronics, used for storage and supply of electrical energy. Electronics, automobiles, home appliances and almost every device need electrical power to operate. Potable batteries, either primary or secondary, come in different sizes with different power capabilities. Primary batteries are most commonly used for single run and important for electronic products i.e. watches, hearing aids. Secondary batteries are rechargeable batteries, widely in demand due to its long life cycle and large energy densities.

In the rapidly growing market, there are different kinds rechargeable batteries, such as Lithium-ions, Nickel- Cadmium (Ni-Cd), Nickel-metal hydride (Ni-MH), and polymers batteries. According to the market survey, by well known firm "SBI energy", of rechargeable batteries; Lithium-ion batteries share about 75% of market, whereas Ni-MH shares about 1.7% of world market in 2008 and will increase to 4.2% in 2013 [61]. Nickel Cadmium was popular in the beginning of 20^{th} century, but due to toxicity of cadmium, it lagged behind in the competition. There are some other batteries, which contribute in rechargeable batteries world market, i.e. Carbon-Zinc, solid polymer etc. The rechargeable batteries based on nonconjugated

conductive polymers discussed here are to lower cost and to provide thin-film capability, therefore, more flexibility in design.

Commercial rechargeable batteries are available in different shape and sizes, which very common small sizes are AA, AAA and 9V. Figure (5.1) compares battery capacities (mWh) of different kind of batteries. Alkaline batteries have greater capacity and nominal voltage. But in rechargeable batteries, NiMH has better result of voltage and battery capacity [61-62].

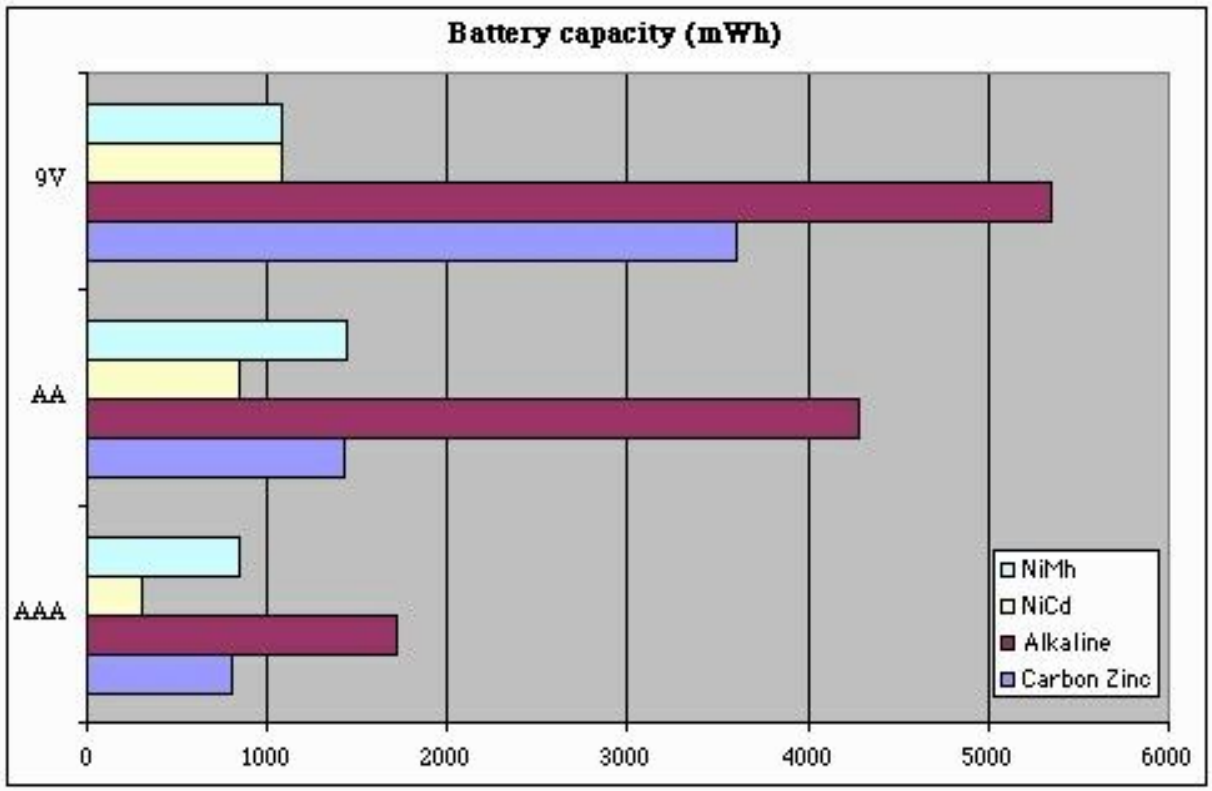

Figure 5.1: Battery Capacity of different batteries [62]

5.1.1 Lead Acid Batteries

Lead acid batteries are the oldest rechargeable battery, widely used in automobile and heavy-duty equipment. Both electrodes in this battery are made of different forms of lead with

sulfuric acid or other mixture, as electrolyte. Although there are so many new rechargeable batteries but lead acid batteries have great impact on rechargeable batteries world and contributed in US rechargeable batteries market, about 79% in 2008.

It has nominal potential 2.0V - 2.1V per standard cell and capacity rate [is 2.5Ah to 25Ah according to the grades in the market [58-59]. It also has higher discharge current due to low impedance and thin lead plate structure. The main problem of lead acid battery is Sulfation, due to formation of crystallized lead sulfate and corrosion of positive electrode and body; it limit the use of these batteries.

5.1.2 Nickel Cadmium Batteries (Ni-Cd)

The miniature world of electrical and electronic devices needs more efficient and compact batteries. Nickel–cadmium rises as new portable rechargeable batteries in different shape and sizes. With high discharge rate and high energy density it made its own place in market and share with lead acid batteries. Because of its compact or small size; it is used in various portable electronics i.e. TV remotes, cameras, lamps.

The nominal capacity of Ni-Cd is in range of 4.5Ah -11.0Ah in 5h and charging and discharging current is in range of 0.9A -2.2A in 7h. But there are some drawbacks of Ni-Cd batteries, which reduce its value in market, such as loss of memory, recycling of Cadmium due to its toxic nature and high cost. [58]

5.1.3 Nickel Metal Hydride Batteries (Ni-MH)

Due to environmental hazardous nature of Cadmium, it was replaced by metal-hydrid, which gives 3-times more power than Ni-Cd. Recycling of battery depends on metal used and

Nickel can be completely recycled. Nominal charge capacity range at 1.2V/cell is 1100mA.h – 3100mA.h and its self-discharge is about 30% per month. Due to low cost and lightweight, it is used in satellite electronic application.

5.1.4 Lithium-Ions Batteries (Li-ion)

Most popular rechargeable battery is lithium-ion battery. It comes in different shape and sizes according to compactness devices, i.e. cameras, cell phones, laptops. There are various ion-electrode combinations that can be formed with lithium electrodes. Such as, lithium sulphur dioxide that has a capacity of about 20-100Ah at 12V and self-discharge rate is 10% per month [59-62]. Recently, lithium has been combined with nano-composite cathode, sulphur/mesoporous carbon, which imparts higher energy capacity to the battery, more than 4-times in contrast to a conventional battery [76].

5.2 Nonconjugated conductive polymer battery

The major motivation of using nonconjugated conductive polymers as electrodes in batteries, is, their significantly lower materials-cost and ease of processibility. The nonconjugated conductive polymer, iodine-doped cis-polyisoprene (natural rubber) has been used as positive electrode for rechargeable batteries. The characteristics and properties of cis-polyisoprene (CPI) have been discussed in chapter 4. It becomes conductive after doping with iodine; shows strong absorption and large nonlinear properties after doping.

Due to increase in conductivity by many order of magnitude upon doping, doped CPI used as electrode (positive) in rechargeable battery. It has been tested with different combinations of counter-electrodes and electrolytes.

5.3.1 Electrolytes

Two types of electrolytes have been used in cis-polyisoprene battery. One is the solution of sodium chloride (NaCl) in water and other is the solution of sodium chloride in ethylene glycol. An additive, known as polyvinyl alcohol (PVA), was added in electrolyte solution, in range of 0-50% by weight of NaCl. Viscosity of electrolyte increases with increase in amount of PVA in the solution and make it in gel form. It also slightly increases the resistance of the battery

5.3.2 Negative Electrode

Two types of negative electrodes, have been tested by Veera [77] in Photonic Material Research Laboratory; zinc and aluminum for potassium iodide rechargeable battery. Zinc gives good potential difference, but it had to be protected for longer duration of operation. In contrast, aluminum was less stable. In this work, NaCl electrolyte was used with negative electrodes of stainless steel in the form of thin strips of dimensions of ~ 20mmx5mm.

5.3.3 Positive Electrode

Cis-polyisoprene (CPI) is used as positive electrode in NaCl rechargeable battery. Latex (natural rubber) is dissolved in water; deposited on glass slide to make thin film of CPI and then it was doped with iodine for 12- 16 hours. After doping, it becomes highly conductive and the maximum conductivity is 0.1S/cm. The dimension of the film is depending on the size of battery. To make cathode, thin film of doped CPI on glass slide of dimension 18cm × 6cm, coiled by thin platinum wire as show in Figure (5.2).

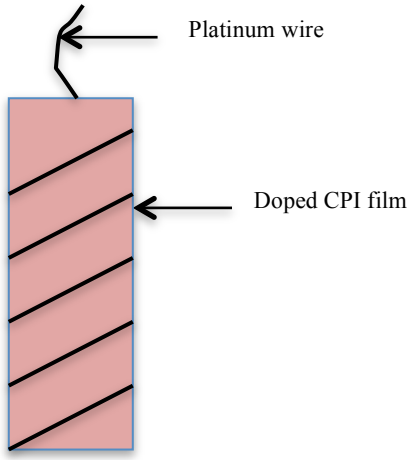

Figure 5.2: Positive Electrode made by doped cis-polyisoprene

Any wire can be use to connect with power supply or multimeter. Platinum has higher potential difference than commonly used wire, i.e. copper, aluminum.

5.3.4 Packaging and measurement

Packaging is the most important step for making a battery; performance depends on packaging directly or indirectly. The glass bottle is used for packaging; filled with electrolyte to $3/4^{th}$ of height of bottle. Both electrodes, anode and cathode, were attached to the cap of bottle at certain distance. It is important to make sure that both electrodes shouldn't touch each other, inside and outside of the bottle. Platinum lead connected to the polymer electrode acts as the positive terminal and steel electrode acts as the negative. A multimeter is used to record the current and voltages as shown in Figure 5.3. To prevent leakage of charge and evaporation of electrolyte through electrode and cap, all lining and holes were secured by strong duck tape or wax.

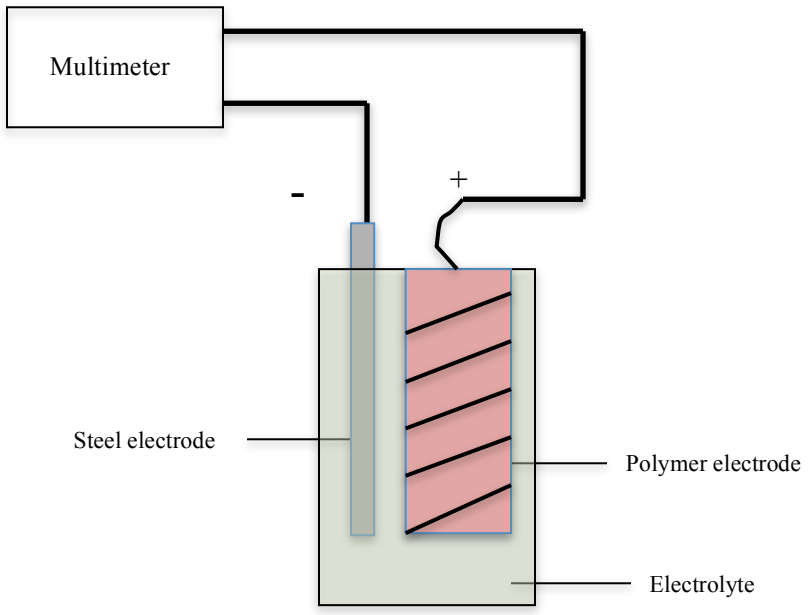

Figure 5.3: Doped CPI battery

5.3.5 Results and Discussion

The measurements of current and voltage were done at three different percentage of PVA in electrolyte solution and discharge current rate were plotted. Without charge, CPI battery gives 0.2V potential difference and current was in the range of microns. After being charged by power source at 5V for 5mins. Electrolyte with ethylene glycol solvent gave a potential difference of 2.0V, but didn't stay for more than 10 minutes. Thus, electrolyte with water found better than with ethylene glycol.

The potential difference increases to 1.5 V and current to 3mAfor the case of NaCl (with water) electrolyte without PVA (0% of PVA). But it didn't last for more than 30 minutes and also current dropped sharply within 3minutes from 3mA to 0.5mA. Figure 5.4 showing discharge current rates for three electrolytes with 0%, 30, and 50% of PVA by weight of NaCl in solution.

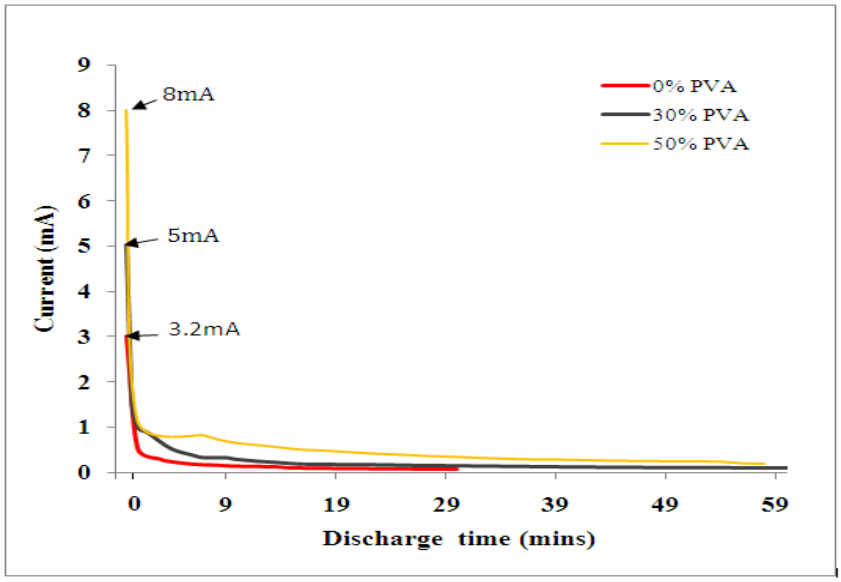

Figure 5.4: Current discharge rate for different percentage of PVA

As percentage of PVA increases, battery current and its discharge rate also decreases. In Figure 5.4, comparing current and discharge rate for 60 minutes; 30% of PVA gave 5mA at 1.58V whereas 50% of PVA induced 8mA at 1.6V. There has not been seen much difference in voltage or potential difference of the battery after adding of PVA.

These batteries have been studied for number of recharge cycles and for series connection. After recharging batteries at same 5V for 5minutes, similar results were obtained, as seen in Figure 5.5, which demonstrates two charging and discharging cycles for 50% of PVA. Upon recharging, it shows current about 8.5mA, at 1.6 V without significant change in discharge current rate.

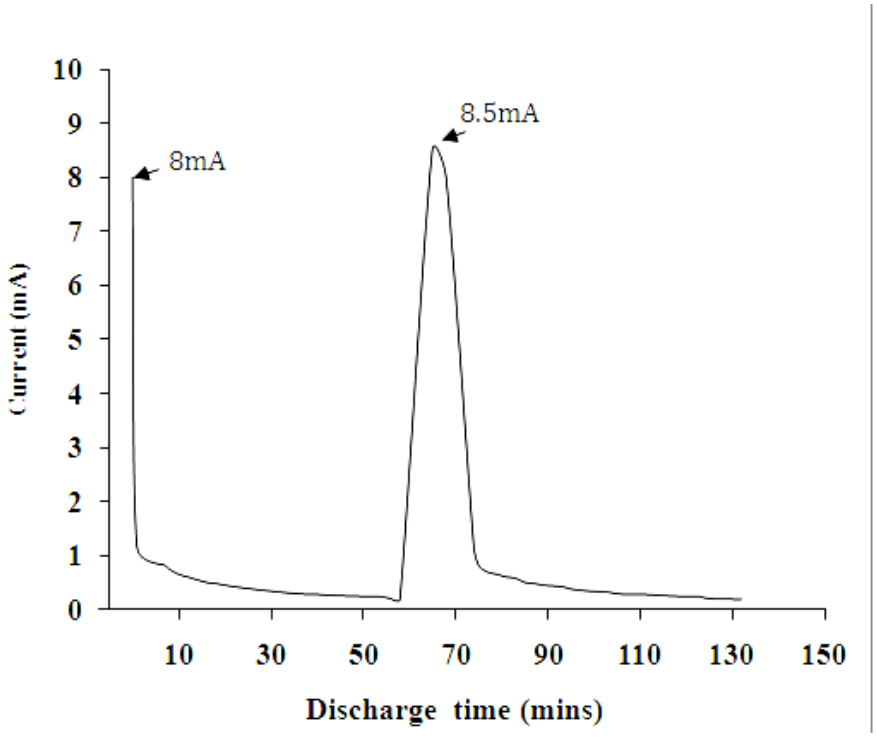

Figure 5.5: Two recharging cycle of Battery for 50% PVA at 1.6V

Series connection of batteries has been tested, i.e., two batteries connected together in series connection and potential difference recorded on multimeter was found to be just double of voltage provided by single battery. This implies that as many as batteries can be connected in series as per the requirement of voltage.

5.4 Conclusion

Doped nonconjugated conductive polymer was used as cathode and steel as anode for making rechargeable battery. NaCl was used as an electrolyte along with PVA as an additive at different percentage levels, ranging from 10-50% by weight of NaCl. The results indicate that, the additive PVA cause leads to gradual slow down in discharge rate and increase in batter life from 30 mins. to 130mins. The best result obtained at 50% PVA concentration in electrolyte that gave a potential difference of 1.6V along with maximum current of 8mA. The potential

differences obtained from both electrolyte of CPI battery are larger than Ni-Cd and Ni-MH batteries. The most important advantage of NaCl battery is low cost of materials and fabrication of battery.

CHAPTER 6

QUADRATIC ELECTRO- OPTIC EFFECT AND STRUCTURAL STUDIES OF TRANS-POLYISOPRENE

6.1 Introduction

Materials and structures of confined dimensions are important for fundamental studies and various novel technological applications. Nonlinear optical characteristics were known to substantially enhanced for confined electronic systems [1-3,6,12]. Among organic materials, conjugated polymers are known as quantum wires because of one-dimensional delocalization of electrons. Recently, nonconjugated conductive polymers have been shown to have quantum dot characteristics because of the confinement of charges within subnanometer domains. Such confinement has led to significantly larger third order optical nonlinearities for these systems compared to known materials and structures.

Quadratic electro-optic effect in nonconjugated conductive polymers including cis-polyisoprene, poly(b-pinene), poly(ethylenepyrrolediyl) derivative and polynorbornene have been recently reported [1-3,12]. Exceptionally large Kerr-coefficients (about 30 times that of conjugated polymers) have been observed in these systems [77]. In the present article, we discuss quadratic electro-optic measurement in the nonconjugated conductive polymer, iodine-doped trans-polyisoprene. As reported back in 1988, cis- and trans-polyisoprene both become electrically conductive upon doping with electron acceptors such as iodine.[7] The conductivity increases by eleven orders of magnitude to a value ~ 0.1 S/cm. The trans- conformation (gutta percha) is semicrystalline as opposed to the cis- conformation (natural rubber) which is

predominantly amorphous. Therefore, trans-polyisoprene is mechanically stronger compared to cis-polysoprene and is without the unique rubber elasticity that cis-polyisoprene (with slight modification) has. In this report, we discuss structural and nonlinear optical property, in particular, quadratic electro-optic effect in doped trans-polyisoprene film

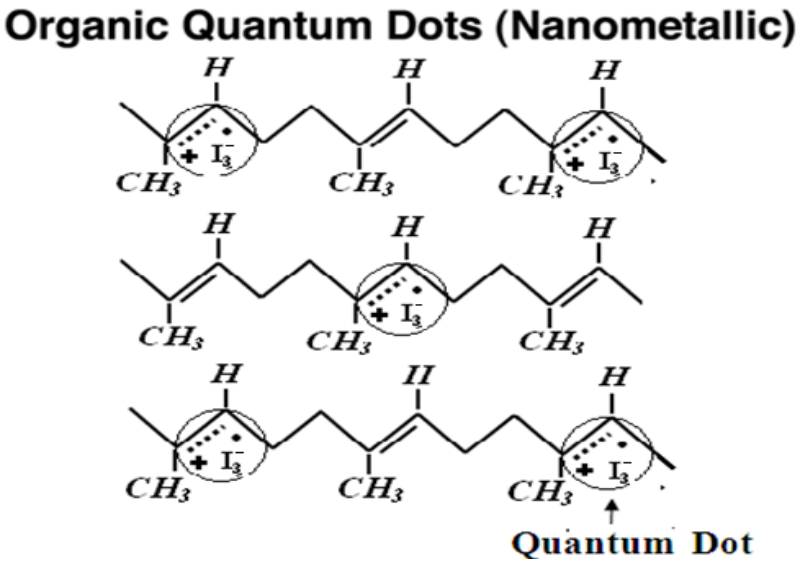

Figure 6.1: Transformation of double bond into cation radicals

Positive charge and cation radicals are confined near double in a subnanometer domain as shown in Figure 6.1, which is less than a nano-scale. Trans-1,4- polyisoprene has studied by optical absorption, FTIR spectroscopy and X-ray diffraction and its electro-optic effect has been measured

6.2 Optical Absorption

Optical absorption of trans-1, 4-polyisoprene has been conducted at various doping level. Sample made on glass slide absorption has recorded Absorption spectrometer Undoped trans-polyisoprene was clearly transparent as shown in Figure 6.2, but after doping it shows two peaks,

one due formation of radical cations at 4.2 eV and second due to charge transfer double bond to dopants (electron acceptors) at 3.1 eV

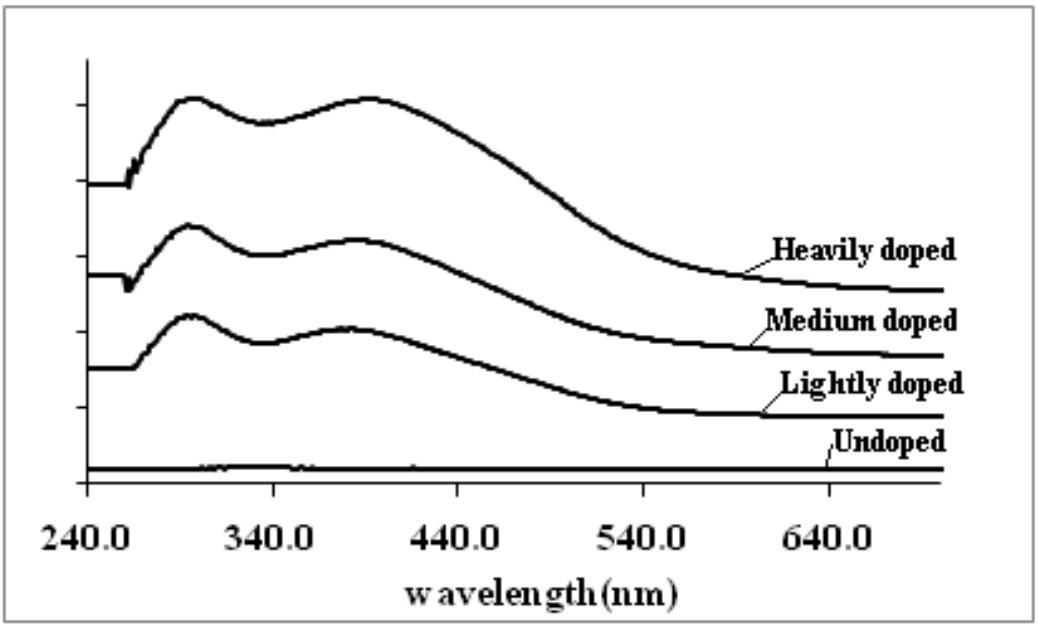

Figure 6.2: Optical absorption of trans-polyisoprene

As concentration of iodine increases, peaks increases and peak correspond to 3.1 eV get broaden and undergoes redshift due to reduction in separation distance between donor and acceptor. The optical absorption of silver nanocrystal has shown in Figure 6.3, absorption peak depends on size of nanoparticles; it increases with increase in size of particles [78]. Non-conjugated polymers have comparable optical absorption spectrum to the nanometallic absorption spectrum. The peaks of silver nanocrystal is at 425nm whereas due to charge of trans polyisoprene confined in subnanometer domain, peaks are at less than 400nm and also define nanometallic or quantum dot characteristics of trans 1,4-polyisoprene.

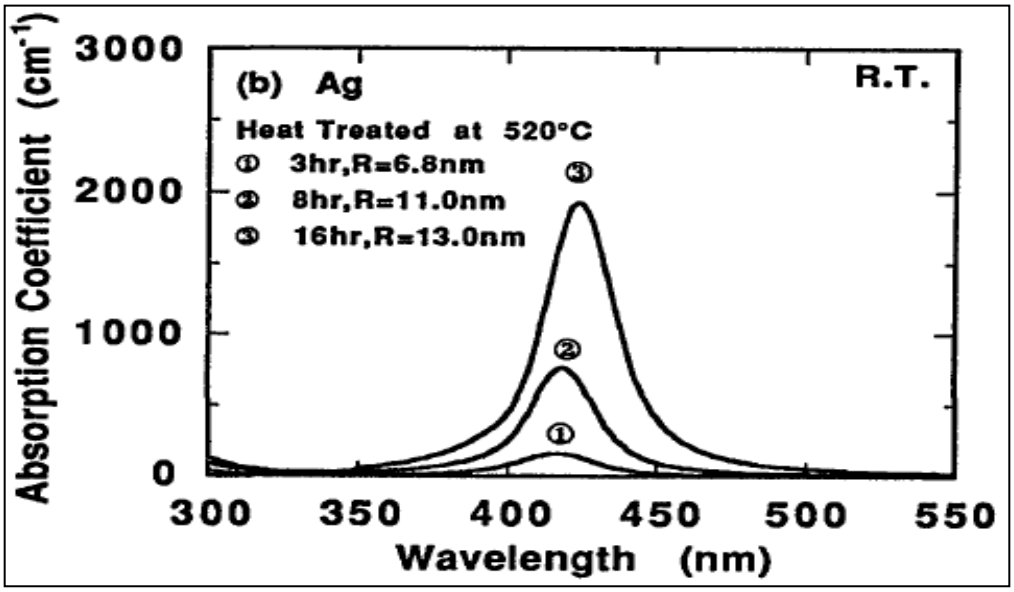

Figure 6.3: Optical Absorption of Silver Nanocrystal

6.3 FTIR Measurement

Conductivity of non-conjugated polymer depends on breakdown of double bond into radical cation and charges [63-64,66]. FTIR spectroscopy studies carried out for undoped and iodine doped trans-1,4-polyisoprene. Sample were mode on KBr pellets and spectra obtained by using 5PC FT_IR spectrometer. Absorption spectra corrected for water. Spectra shows for specific range in Fig(11) which has peak at 799cm^{-1} due to bending vibration of =C-H bond in undoped trans-poly isoprene, doping leads to a reduction of peak due to formation radical cation and charge transfer and it directly proportional to iodine concentration

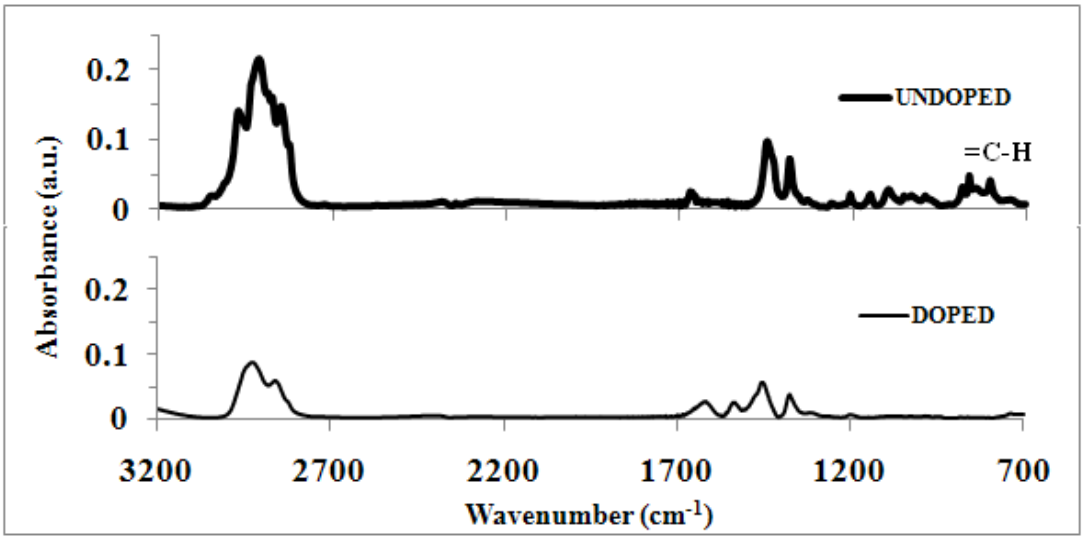

Figure 6.4: FTIR spectrum of undoped and doped trans-polyisoprene

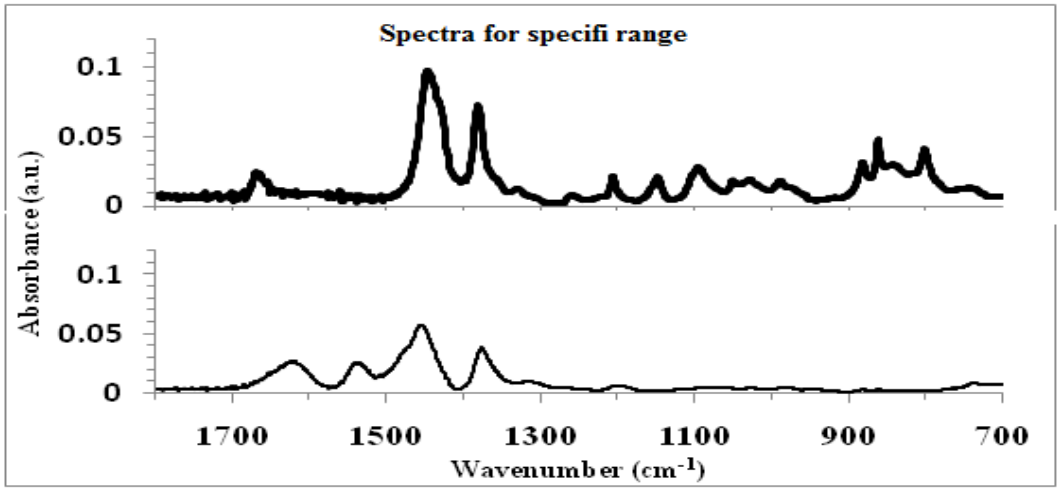

Figure 6.5: FTIR spectrum of undoped and doped trans-polyisoprene for specific range

6.4 Structural Studies of Trans-polyisoprene using X-ray Diffraction

Thin films of trans polyisoprene have been examined under the microscope which shows that the pure trans polyisoprene is polycrystalline shown in Fig.7, which is not good for quadratic electro-optics. It was accidentally found that on addition of C60 (fullerene) in a very small fraction in trans-polyisoprene very smooth and excellence surface of the films for electro-optics

as shown in Figure 8 are obtained. Crystal structure of trans-polyisoprene was studied in detail in the past and three-phase α, β, γ forms were found in 1940s. In 1942 Bunn reported detailed crystal structure of the γ form (orthorhombic) with unit cell parameters:

a = 7.78, b = 11.78A and c = 7.75A γ=94^o **[17,18]**

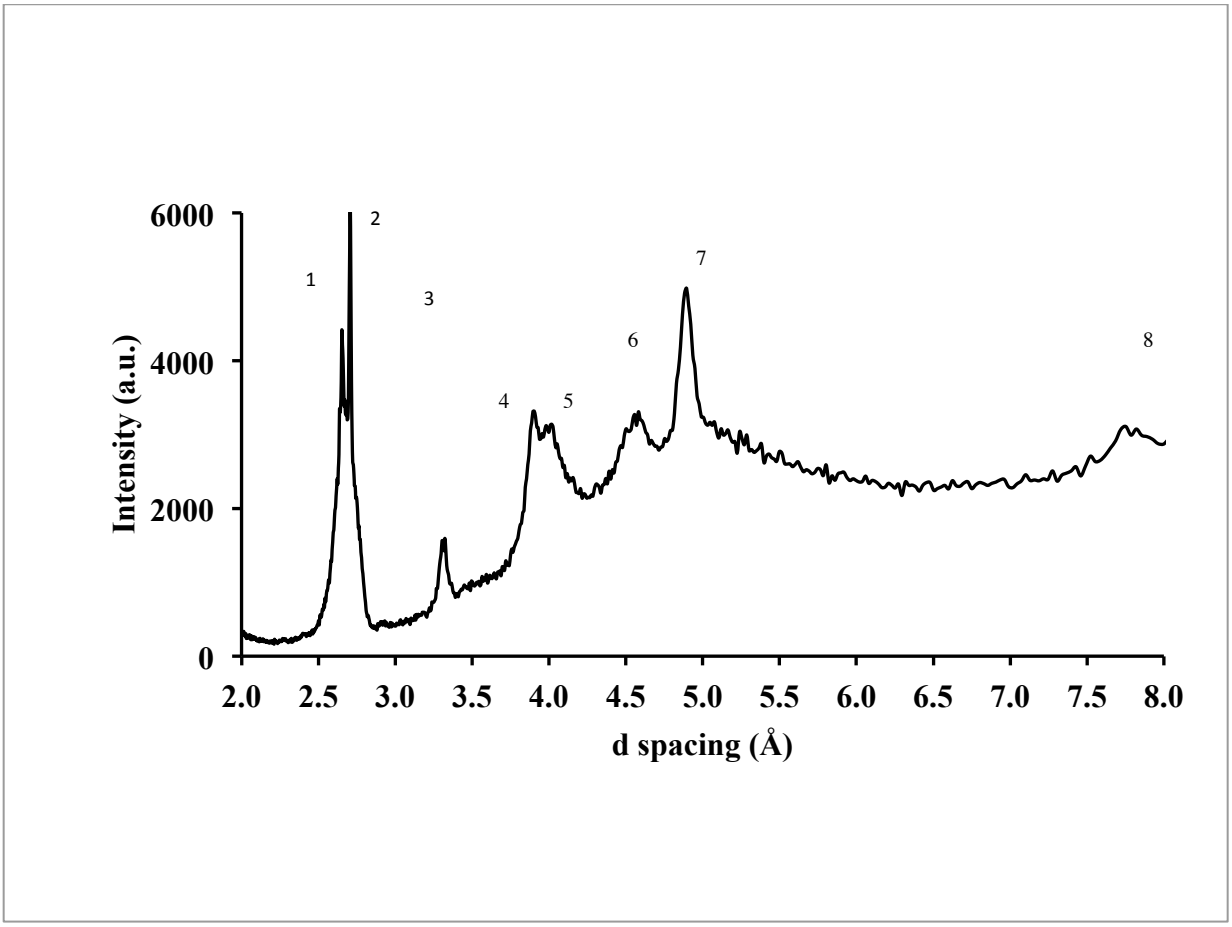

Figure 6.6: X-Ray diffraction of undoped trans-polyisoprene

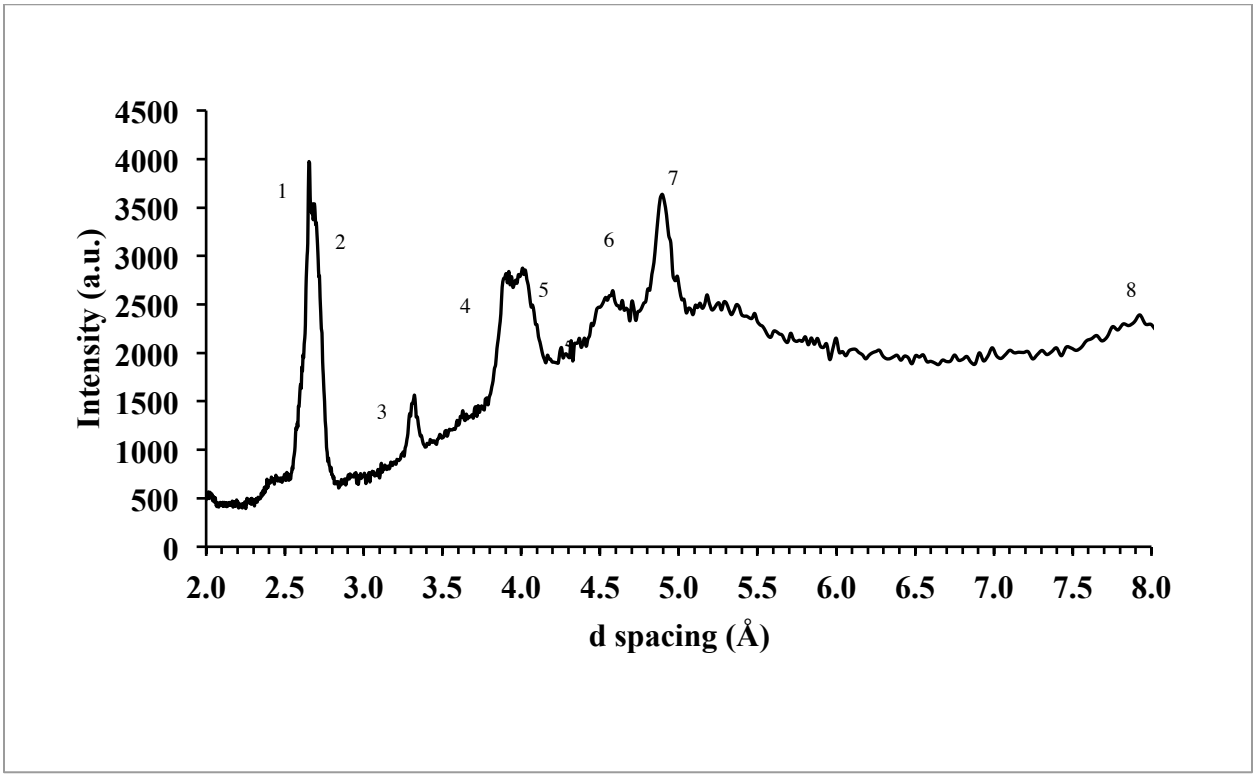

Figure 6.7: X-Ray diffraction of trans-polyisoprene after doping with iodine

Miller indices have been calculated corresponding to d-spacings, (Table 6.1) which shows the γ phase of trans-polyisoprene, reported by *Rootare et.al.* (1977) [20

Table 6.1:Miller indices of TPI with d-spacing

Peaks	d-spacings (Å) undoped	d-spacings (Å) doped	Miller Indices
1	2.683	2.653	122 ↑
2	2.707	2.687	210 ↓
3	3.366	3.326	112
4	3.904	3.904	020
5	4.054	4.008	111 ↑
6	4.582	4.582	110
7	4.895	4.895	010

The results of x-ray diffraction measurements are shown in Fig.6.6 and 6.7. These results clearly show that trans-polyisoprene is polycrystalline [82]. The d-spacings show that the film has structure of γ-phase of trans-polyisoprene [17-20]. The γ-phase has lattice parameters: a = 5.9A, b = 7.9A, c = 9.2A and $\gamma = 94^{o}$. The Miller indices of the peaks for the undoped and doped films (molar concentration of iodine ~ 0.5) are shown in Table 6.1. The peaks, (1 and 5 in Table 6.1) including (122) and (111) were increased in intensity upon doping. The second peak (210) slightly decreased in intensity upon doping. The rest of the peaks and the d-spacings of all the peaks within the range considered were unchanged upon doping. This leads to the suggestion that iodine atoms are closer to the (111), (122) planes within the unit cell of trans-polyisoprene and that caused the increase in intensities of the corresponding peaks. Similarly, little or no changes in d-spacings were observed upon iodine doping of the conjugated polymer polyacetylene compared to the undoped state [79]. More detailed work needs to be done to look into the crystal structure of doped trans-polyisoprene

6.5 Sample Preparation for Electro-optics

Trans-polyisoprene has polycrystalline behavior, sample film of TPI is not smooth, it restricts electro-optics. We added very small fraction fullerene (C60) with TPI in an organic solution toluene and kept at 50^{o}c. Sample film shown in Figure 8, got from the new solution, very smooth and gives good electro-optic response.

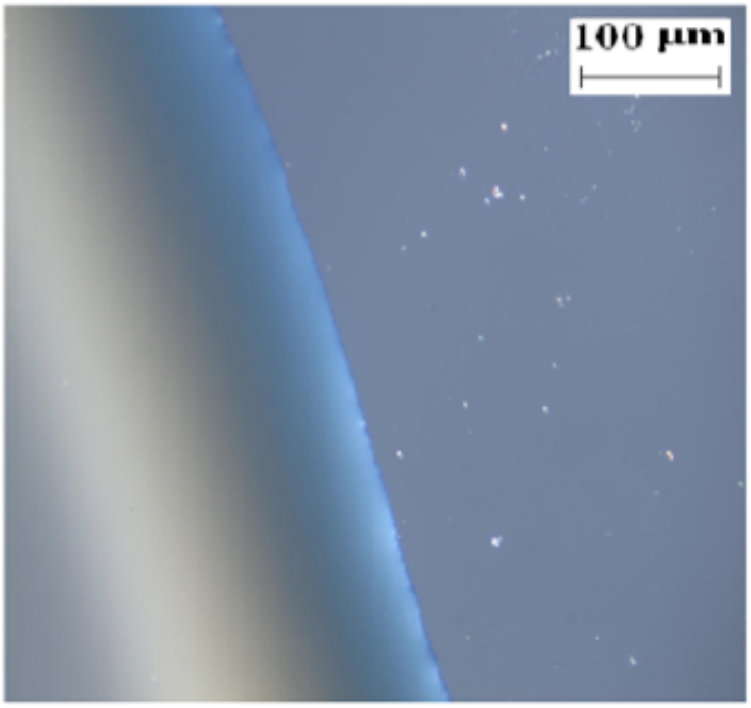

Figure 6.8:Micrograph of trans-polyisoprene with C60

Two copper tape stick on a glass slide, parallel to each other with slit width 100µm-300µm. Sample place on copper slit, which induce electric field, when connected to AC power

6.6 Electro-Optic Measurement

The sample of trans-polyisoprene film was doped with iodine and it was studied for non-linear / electro-optic measurements at 633nm and 1550nm wavelengths [82]. The measurements have been made in the cross polarized geometry using field induced birefringence (Fig.6.9). A laser beam polarized at 45^{o} with respect to applied electric field is passed through the sample and an ac field at 4kHz is applied. The resulting modulation due to quadratic electro-optic effect is recorded in a lock-in-amplifier (with 2f synchronization) and an oscilloscope.

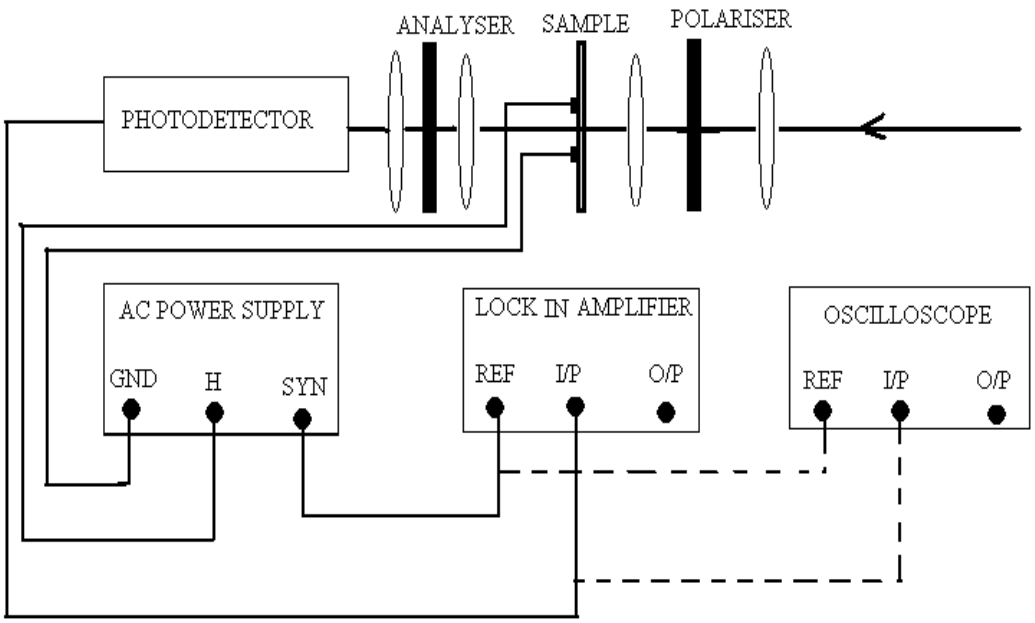

Figure 6.9: Experimental Setup for electro -optics

6.7 Result and discussion

Electro–optics had performed on field induced birefringence setup shown in Fig.6.9. Output has been detected by photodetector, read on lock-in-amplifier and quadratic waveform has seen on oscilloscope, in Figure 6.9.

Modulation depth of average 0.14%has been observed for an applied field of 1.1 V/μm for a 0.37μm thick film, which is much higher than the modulation depth of other non-conjugated polymers. The modulation depth had a quadratic dependence on applied field as shown in Figure 6.10.

There are two forms of natural rubber, one is cis-polyisoprene and other is trans-polyisoprene. Both of them show exceptionally large nonlinearities and quadratic effect. Cis-polyisoprene have third order susceptibility and Kerr coefficient of 3.4×10^{-8} esu (Estd.) and 1.6×10^{-10}m/V^2 respectively whereas trans-polyisoprene has a higher nonlinearities such as third order susceptibility and Kerr coefficient are 5.6×10^{-8} esu (Estd.) and 3.5×10^{-10}m/V^2 respectively

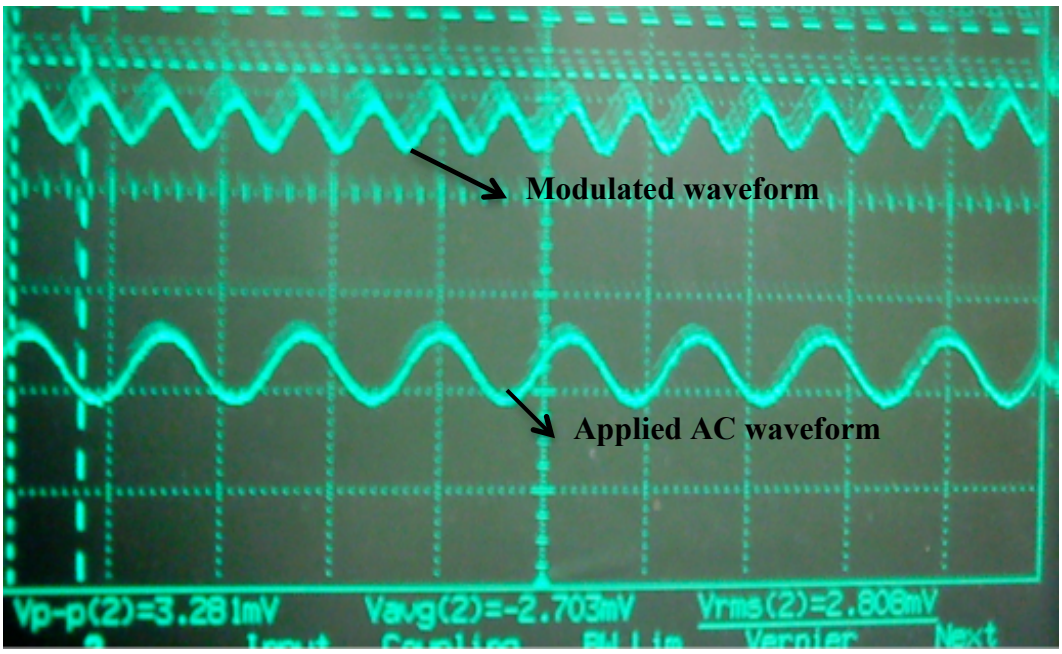

Figure 6.10: Oscilloscope trace of modulation

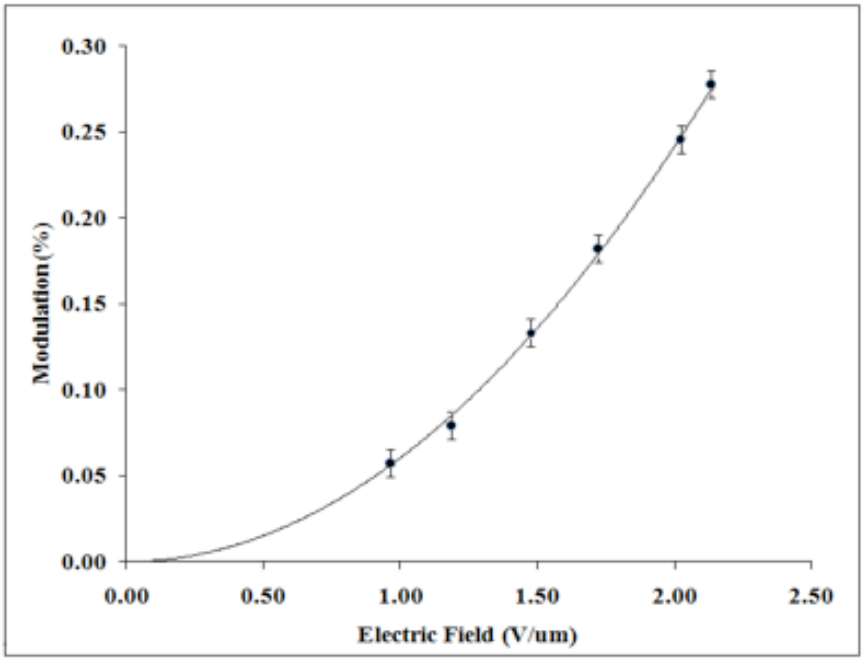

Figure 6.11: Quadratic modulation depth due to applied Electric field

Comparison of nonlinearities has been shown below in Table (6.2) with some other polymers and nano-metals.

Table 6.2: Comparison of third order nonlinearities

Material	**Wavelength (nm)**	**Kerr coefficient** (m/V^2)	**$\chi^{(3)}$ (esu)**
PTS-polydiacetylene	1550	$3x10^{-12}$	$5x10^{-10}$
Poly β-pinene	633	$1.2x10^{-10}$	$2.6x10^{-8}$Estd.
Cis –polyisoprene	633	$1.6x10^{-10}$	$3.4x10^{-8}$Estd.
Ag-SiO_2	1064	$3.4x10^{-12}$ Estd	$7.3x10^{-10}$ [42]
Cu-$SrTiO_3$	770	$3.0x10^{-13}$ Estd	$6.5x10^{-11}$ [44]
Trans-1,4- polyisoprene	***633***	***$3.5x10^{-10}$***	***$5.6x10^{-8}$Estd.***
Trans-1,4- polyisoprene	***1550***	***$2.5x10^{-10}$***	***$4.0x10^{-8}$Estd***

6.8 CONCLUSION

Quadratic electro-optics effect and X-ray diffraction of trans-polyisoprene have been measured for the first time. The optical absorption spectrum at low doping shows two peaks: one at 4.2eV due to radical cation and the other at 3.2eV due to charge-transfer. Doping leads to a reduction of the intensity of =C-H bending vibration-band due to formation of radical cations upon charge-transfer. Quadratic electro-optic measurements have been made using field-induced birefringence method at 633 nm. A modulation depth of 0.14% has been observed for an applied field of 1.1 V/μm for a 0.37μm thick film. The modulation depth had a quadratic dependence on applied field. The Kerr coefficient as measured is exceptionally large and has been attributed to

the sub-nanometer size metallic domains (quantum dots) formed upon doping and charge transfer.

CHAPTER 7

COMPARISON OF OPTICAL PROPERTIES OF NONCONJUGATED CONDUCTIVE POLYMERS AND NANOMETALS

7.1 Introduction

Nanomaterials have better thermal, electrical and optical properties and are being widely studied for use in various fields, starting from medical use to weaponry for military. Nowadays they are also used to manufacture biosensors and photovoltaic devices. Nanometallic particles have attention-grabbing optical properties (both linear and nonlinear). They have unique pattern of absorption, transmission and color spectrum, which depend on nanoparticles shape sizes and surface. They exhibit a quality of changing of color due to Surface plasmon resonances.

When nanoparticles interact with light, electron and photon excite at different wavelength and start oscillating. This process is known as Surface Plasmon resonance, which causes strong absorption and scattering properties [52-53,79]. The resonance is achieved at specific wavelength and angle (SP angle) and it depends on properties of nanoparticle sample film, frequency of plane polarized light and refractive index of media. The depression relation is given in term of frequency (Eqn. 7.1)

$$K(\omega) = \frac{\omega}{c}\sqrt{\frac{\varepsilon_m \varepsilon_{np}}{\varepsilon_m + \varepsilon_{np}}} \qquad Eqn(7.1)$$

where ε_m and ε_{np} are dielectric constant of media and nanoparticles.

Silver and gold nanoparticles are most commonly known for surface plasma resonance and got attention due to their stability in atmosphere and tunable broad absorption band of wavelengths 400nm(near UV) to 1000nm (near IR).

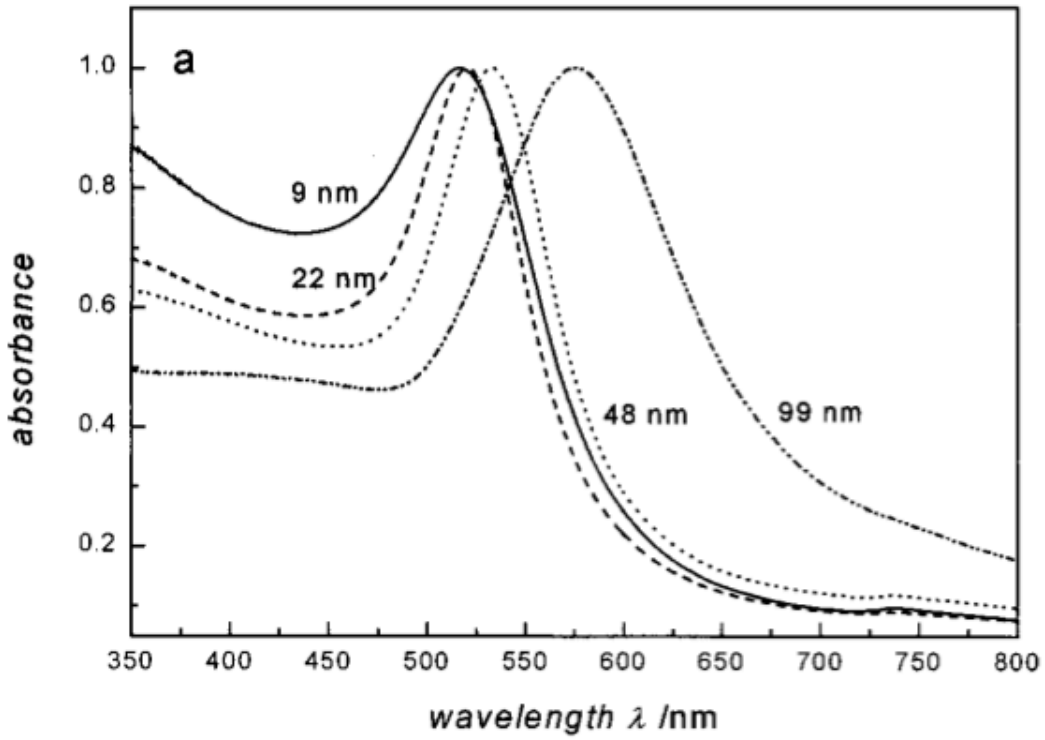

Figure 7.1 Absorption spectra of Gold nanoparticle of different diameters [56]

It has been established that optical properties of nanoparticles are size dependent. Figure 7.1, shows absorption of gold nanoparticles of different diameter. As size of the particle decreases, absorption peak increases. There is shift seen towards shorter wavelength and broadness of peak becoming sharper as going from larger size to smaller. `

When nanoparticles interact with white light, they emits different color lights at different wavelength as a virtue of change in size of particles and refractive index of media due to SPR. There are some other metal nanoparticles, which also show surface plasma resonances, i.e. Copper (Cu), Aluminum (Al).

7.2 Dielectric Constant of metal Nanoparticles

Optical properties such as refractive index and absorption coefficient are related to the dielectric constant. Studies have shown that nanoparticles like Au, Ag and Cu have large real and small imaginary dielectric constants and acquire strong plasmon resonance frequencies with large local field. It has been observed that dielectric constants of nanoparticles depend on size of particles, polarization and interfacial conductivity of particle.

Figure 7.2(a, b) shows real part and imaginary part of dielectric constant of silver nanoparticles, reported by *Jirakorn Thisayukta* in 2004 [54].

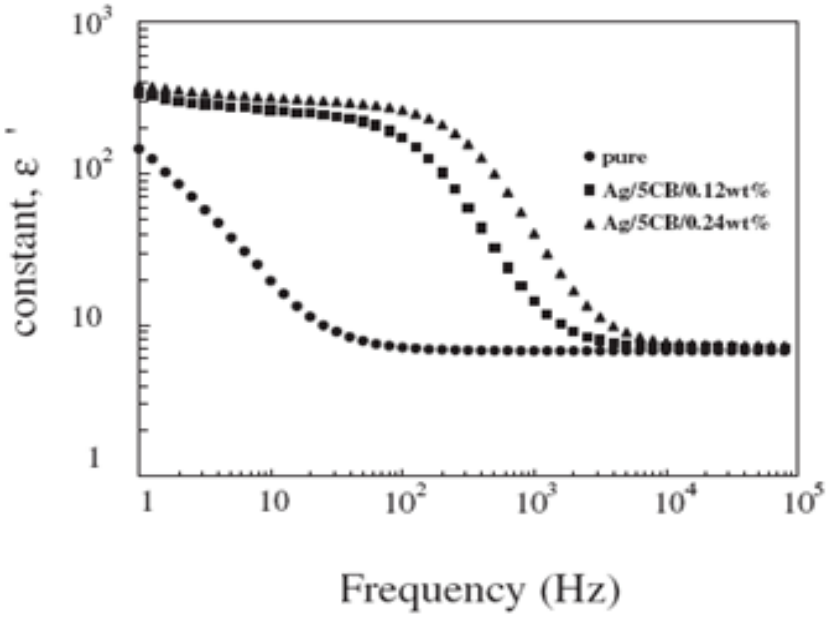

Figure 7.2(a): Real Part of dielectric constant of silver (Ag) nanoparticles

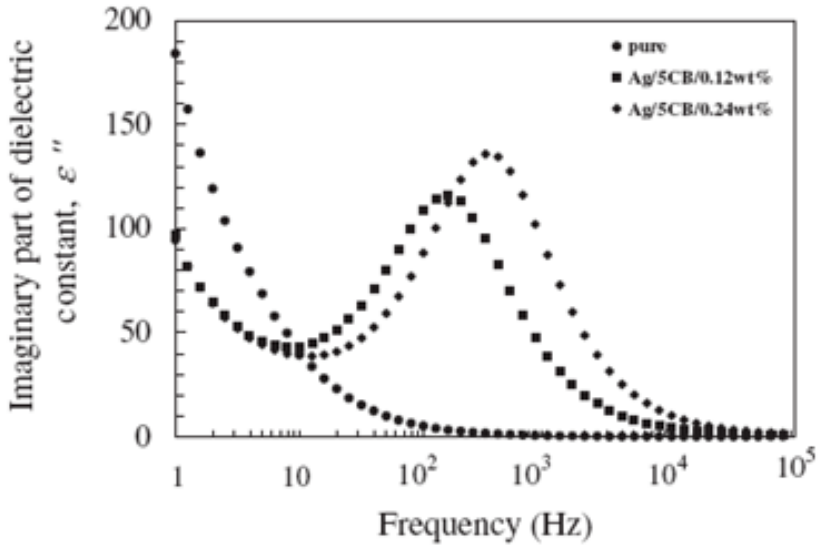

Figure 7.2(b): Imaginary part of dielectric constant of silver (Ag) nanoparticles

It was observed that, dielectric constant increases rapidly with the increase in concentration of NPs. The high imaginary and real dielectric constants as seen in NPs, towards low frequency due to DC conductivity as well as to interfacial polarization is caused by inhomogeneity in the material.

7.3 Nonlinear Properties

Nonlinear optical properties of nanoparticles; Ag, Au and Cu have been studied by many researchers. Higher optical absorption and large nonlinear properties have been seen in nanoparticles. Third order susceptibilities and kerr coefficient were measured by using Z-scan method. Optical absorption for nanometals can be expressed in term of dielectric constant as Eqn. 7.2 [56]

$$\alpha = \frac{18\pi\varepsilon_d^{\frac{3}{2}}}{\lambda}.\frac{p\varepsilon_2}{[\varepsilon_1 + 2\varepsilon_d]^2 + \varepsilon_2^2} \qquad Eqn(7.2)$$

Third order susceptility for nanometals is the function of frequency as given by Eqn. (7.3) [56]

$$\chi^3_{eff} = p\,\chi^3_m \left(\frac{3\varepsilon_d}{\varepsilon(\omega)+2\varepsilon_d}\right)^2 \left|\frac{3\varepsilon_d}{\varepsilon(\omega)+2\varepsilon_d}\right|^2 = p\,\chi^3_m\,(f_c(\omega))^2\,|f_c(\omega|^2 \quad Eqn(7.3)$$

so this states that, at higher frequencies and shorter wavelength nanometals show larger kerr coefficient and third order susceptibilty.

Nonlinear absorption coefficient and susceptibility of copper nanoparticles in 2-Ethoxyethanol with 1% wt. PVP has been reported by *H. H. Huang et. al.* in 1997 [49]. They estimated third order absorption coefficient is about 15 $\times 10^{-10}$ m/W and χ^3 is 4.27$\times$ 10^{-11} esu. χ^3 for copper nanoparticles also reported by *A. Cetin et. al.*, is about 1.55$\times 10^{-10}$ esu [49].

Hideyuki Inouye et. al (1999) studied kerr signal of Gold nanoparticles and estimated it to be about χ^3 = 2.0 x 10^{-8} esu [47]. Nonlinear refraction and absorption coefficient at 532 nm of Au nanoparticles in water; have been studied by *J. T. Seo et.al*. They found nonlinear absorption coefficient and refractive index as -1.89$\times 10^{-9}$ m/W and 4.54$\times 10^{-16}$ m^2/W respectively. The third order susceptibility of gold nanoparticles, in resonant region has been shown in Figure 7.4 [46]

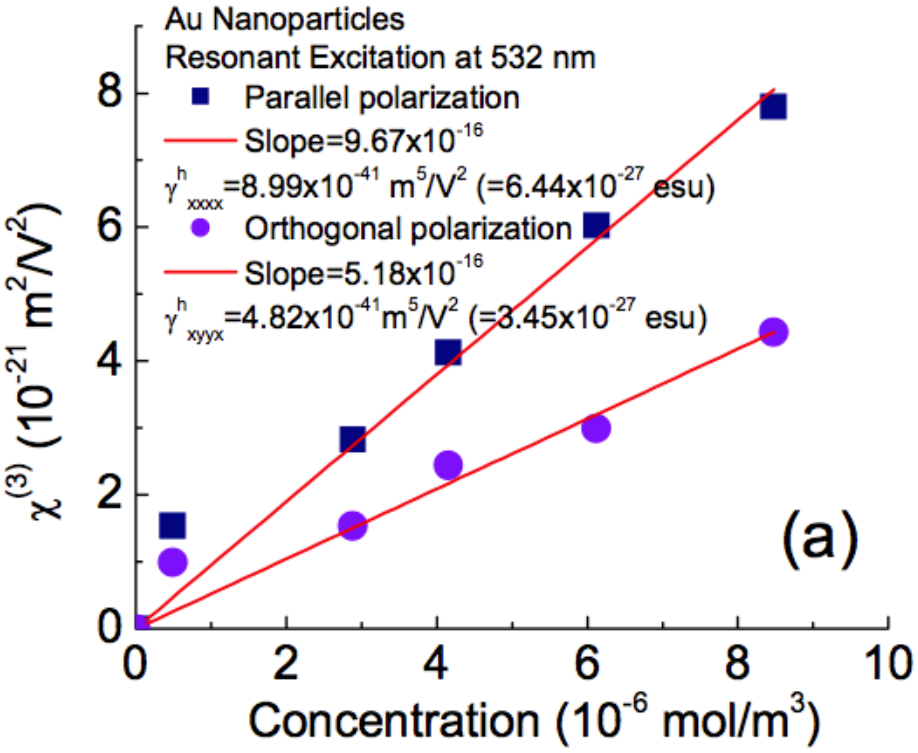

Figure 7.3: Third order susceptibility of gold nanoparticles with molar concentration

7.4 Comparison of Third order Optical Nonlinearities

Nonlinear properties of nanoparticles are applicable to ultrafast telecommunication and other photonic devices. Recent publications and studies have shown that nonconjugated conductive polymers have exceptionally large nonlinear optical properties after doping with electron acceptors. The Kerr coefficients of iodine-doped cis-polyisoprene and trans-polyisoprene were found to be 1.6×10^{-10} (m/V^2) and 3.4×10^{-10} (m/V^2) respectively, which are in the nanometals range [82]. Table 7.1 compares nonlinear properties of nanoparticles of metals and polymers. The nanometallic domains formed in nonconjugated conductive polymers, are shown in Figure 6.1(reproduced for comparison). The encircled regions are subnanometer in dimension.

Table 7.1: Third order nonlinear properties of nanoparticle and polymers

Quantum Dots	**Wavelength (nm)**	**K (m/V^2)**	**$\chi^{(3)}$ (esu)**
Poly(β-pinene)	**1550 nm**	**$1.6x10^{-10}$**	**$3.4x10^{-8}$ Estd**
Cis-polyisoprene	**633 nm**	**$1.6x10^{-10}$**	**$3.4x10^{-8}$ Estd**
Transpolyisoprene	**633nm**	***$3.5x10^{-10}$***	***$5.6x10^{-8}$Estd.***
Poly(ethylenepyrrolediyl)	**633 nm**	**$1.2x10^{-9}$**	**10^{-7} Estd**
Cu : Al_2O_3	**575 nm**	**-----**	**10^{-8}**
Au : SiO_2	**532 nm**	**-----**	**$1.7x10^{-10}$**
PTS-polydiacetylene	**1550 nm**	**$3x10^{-12}$**	**$5x10^{-10}$**

.

CHAPTER 8

STUDIES OF THERMAL PROPERTIES AND ABSORPTION COEFFICIENT OF NONCONJUGATED CONDUCTIVE POLYMER USING SPECIFIC METHODS

8.1 Introduction

Thermal properties, such as specific heat, heat flow rate and phase transition temperatures are important for various applications in thermodynamic and nanotechnology fields. Recently, thermal properties of nanoparticles and polymers have caught attention of researchers for a few decades. Significant enhancements in specific heat capacities have been seen of nanoparticles or nanocrystals than in bulk metal or materials. Differential scanning calorimeter (DSC) is very common instrument, used to study various thermal properties. In this report, thermal properties of nonconjugated conductive polymer, trans-polyisoprene, are studied using DSC.

8.2 Differential Scanning Calorimeter

Differential Scanning calorimeter is conventional instrument used for measuring specific heat capacities, heat flow rate and phase transition temperatures, glass transition (Tg) and melting temperature (Tm). Increase in temperature leads into change in phase of amorphous solids into glassy liquid; referred as glass transition with glass transition temperature (Tg) and it also cause change in specific heat of materials [34,37]. At very high temperature, molecules of amorphous material get freedom to move, convert into crystalline phase. Further increment in temperature cause melting corresponds to melting temperature (Tm) [81]. Glass transition and melting temperatures can be seen in DSC Plot in Figure (8.1)

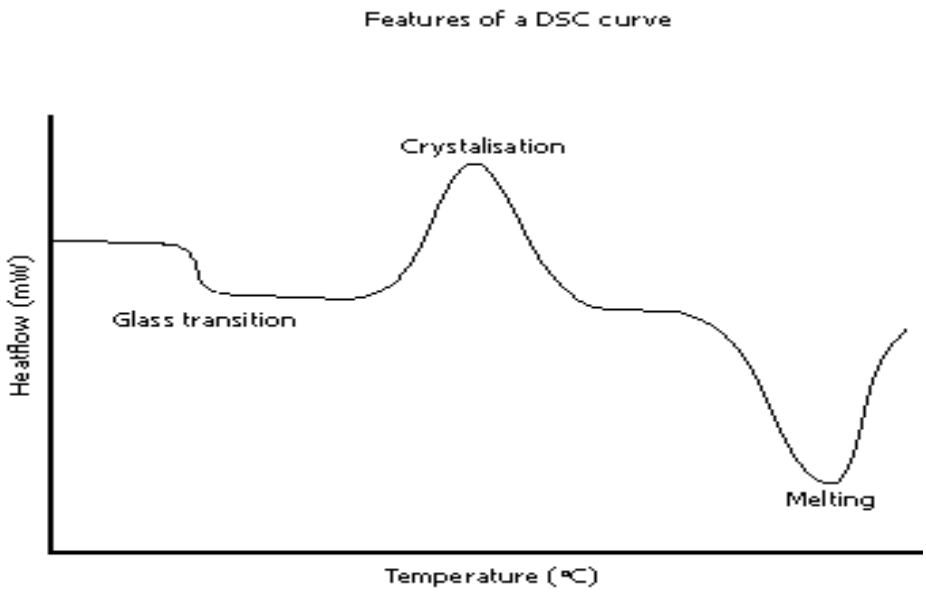

Figure 8.1: DSC plot of heat flow vs. temperature in a material

8.2.1 Specific heat of Nanoparticles

Studies of thermal properties of various semiconductor and nano-sized particles have shown, that they possess higher specific heat capacity than composite bulk material about 10-12 times [35]. J.Rupp group (1987) has reported, that two nano-crystalline metal particles, Cu and Pd, have higher heat capacity compared to polycrystalline metals. Nano sized particle have greater atomic vibration at high temperature, which leads increase in specific heat capacity [36]

Particles size and density cause variation in heat capacity. Softer nanocrystalline particles have greater atomic vibration than microscopic particles, thus, they have higher heat capacity. Thermal properties of CuO have studied by R. S. Prasher, el. at. [37], which state that, the shape of particles also does matter for heat capacity. It has been seen that cubic and thin particle have greater heat capacity.

8.2.2 DSC of Trans Polyisoprene

Thermal properties of nonconjugated polymers, trans-polyisoprene were measured using Differential scanning calorimeter (DSC), before and after doping with iodine. Studies of thermal properties of nonconjugated conductive polymers are still in progress. Just trans-polyisoprene has been discussed in this report. Heat flow and specific heat measurement have been done on specific temperature range from -50^{0}C to 110^{0}C. Melting temperature peak of undoped trans-polyisoprene has been seen at 60^{0}C, which was also reported by *Huafeng Shao et al* [40] for TPI with crystallinity about 50- 60% and Edward G. *et al* also suggested in 1971 that, melting temperature (Tm) for low melting polymer is about 64^{0}C [38-39].

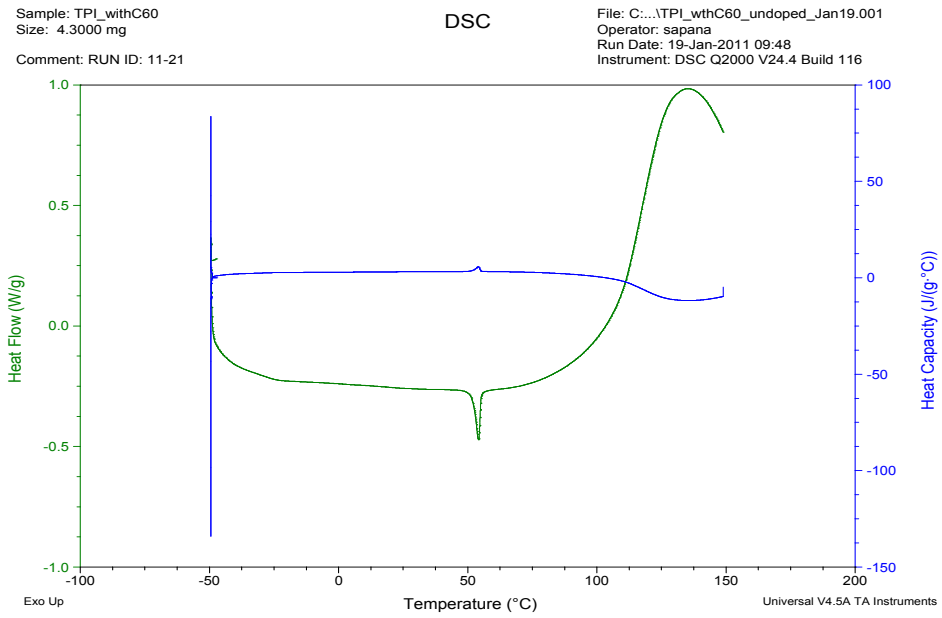

Figure 8.2: DSC scan of undoped trans-polyisorene

Melting peak can be seen clearly in Figure 8.2 at 60^{0}C, whereas after doping with iodine melting point was not well defined. Specific heat of trans-polyisoprene increased after doping with iodine. Figure 8.3(a, b) shows heat capacity and heat flow of undoped and doped tans-polyisoprene for temperature range 10-30 ^{0}C.

Trans-polyisoprene possesses nanometallic and crystalline characteristic, as discussed in chapter 6. Its specific heat capacity is comparable to nanocrystalline particle, which increase after doping with iodine, due to increment in cation radicals. Thickness of TPI sample (0.37μm) and estimated size of particles are less than 1nm, thus lead to higher thermal properties.

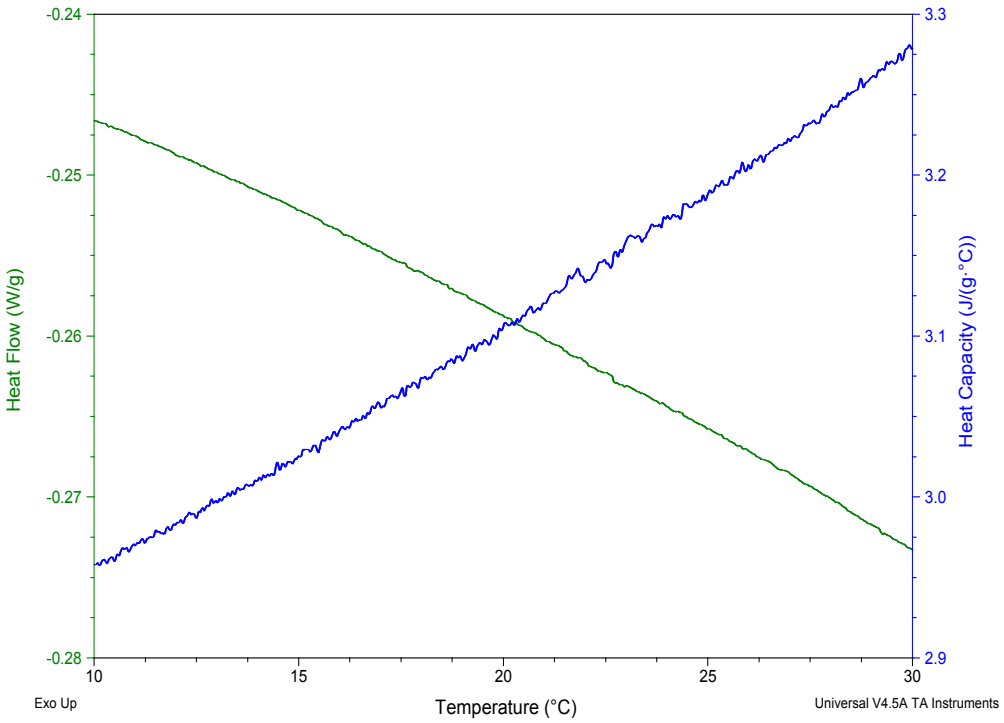

Figure 8.3(a): Thermal Properties of undoped Trans-polyisoprene

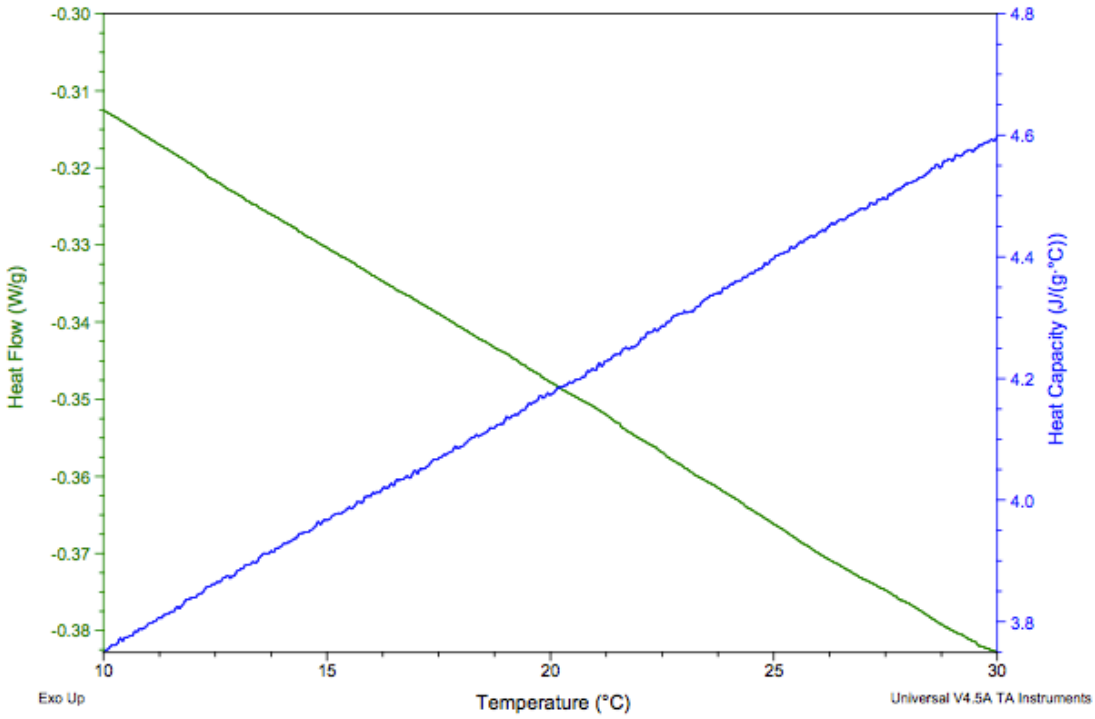

Figure 8.3(b): Thermal Properties of doped Trans-polyisoprene

.

8.3 Refractive index

The relationship between input-output intensities ratio and absorption coefficient is given by

$$\frac{I}{I'} = e^{-\alpha l} \qquad Eqn\ (8.1)$$

Absorption coefficient can be deduce from Eqn.(8.1)

$$\alpha = \frac{\ln(I) - \ln(I')}{l} \qquad Eqn(8.2)$$

where *I* and *I'* are output and input intensities of light and '*l*' is distance travel by light, which is thickness of sample in our case. Eqn.(8.2) is used to calculate absorption coefficient from absorption data.

Optical absorption and refractive index of trans-polyisoprene have been studied. As already discussed in chapter 4, conductivity of trans-polyisoprene increases by many order of magnitude upon doping with iodine. Absorption was studied at different doping level of trans-polyisoprene with iodine. Absorption of trans-polyisoprene showed two peaks after doping with iodine, one at 3.1eV due to charge transfer from double bond to dopant or iodine, second at 4.2eV due to formation of cation radicals. As iodine level increases in polymer, more and more double bond transfer into cation radicals, which cause strong absorption and gives higher absorption coefficient.

The Figure 8.4 shows, absorption coefficient with respect to energy for heavy doping of trans-polyisoprene, absorption coefficients of two peaks are more than 2×10^5 cm^{-1}. High absorption attributed nanometallic characteristics in nonconjugated conductive polymer trans-polyisoprene.

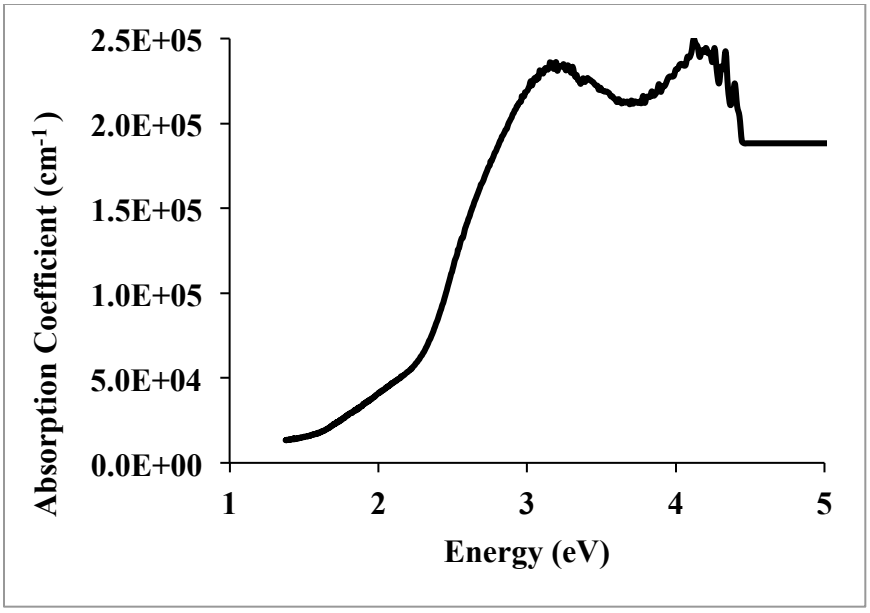

Figure 8.4: Absorption coefficient of trans-polyisoprene at heavy doping with iodine

The refractive indices of iodine doped trans-polyisoprene have been calculated by numerical integration using Kramers-Kronig transformation, which is shown in Eqn.(8.3)

$$n(E) - 1 = \frac{ch}{2\pi^2} P \int_0^{\infty} \frac{\alpha(E')}{(E')^2 - (E)^2} \, dE' \qquad Eqn(8.3)$$

Kramers-Kronig has given refractive index in term of absorption coefficient, which is the function of energy. Numerical integration has done by using MATLAB software. Figure 8.7 is the plot generated by MATLAB, refractive indices with respect to energies, there is increase in refractive indices, that has been seen after doping with iodine.

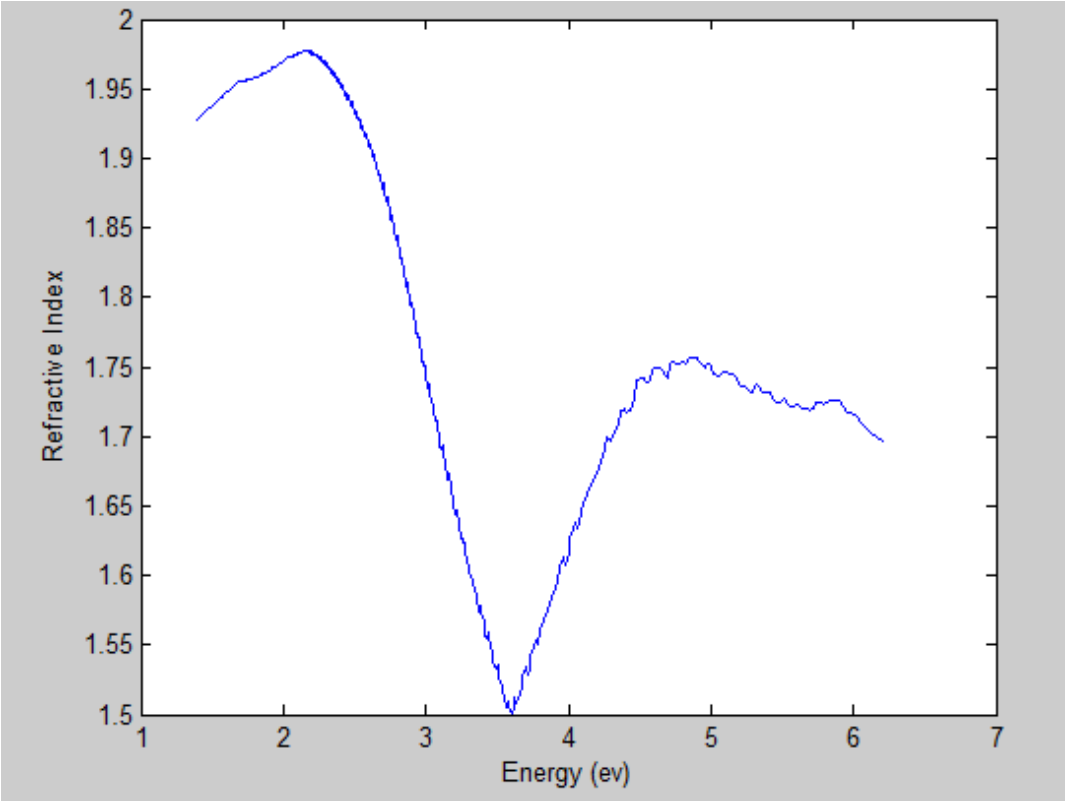

Figure 8.5: Refractive index of heavily doped trans-polyisoprene

8.4 Conclusion

Absorption Coefficients of Nonconjugated Conductive Polymers before and after doping have been determined. Refractive indices of doped poly(β-pinene), cis-polyisoprene and trans-polyisoprene have been calculated by Kramers-Kronig transformation using absorption data Very large absorption coefficients have been observed for doped nonconjugated conductive polymers. Such large absorption coefficients and the wavelength of the maxima are consistent with structures involving subnanometer-size metallic domains. These linear optical constants are important to determine considering exceptionally large Kerr coefficients/third order susceptibilities of nonconjugated conductive polymers

CHAPTER 9

SUMMARY

In summary, molecular and crystal structure of the nonconjugated conductive polymer, trans-1,4-polyisoprene has been studied before and after doping with iodine. Quadratic electro-optic effect has been measured in the doped films. Use of nonconjugated conductive polymer as an electrode in a rechargeable battery has been investigated.

The optical absorption spectrum of trans-1,4-polyisoprene at low doping of iodine shows two peaks: one at 4.2eV due to radical cation and the other at 3.2eV due to charge-transfer. Doping leads to a reduction of the intensity of =C-H bending vibration-band due to formation of radical cations upon charge-transfer. X-ray diffraction data indicated the γ-phase crystal structure for undoped trans-polyisoprene. Upon iodine-doping intensities of specific diffraction peaks slightly increased but the d-spacings of all the peaks remained essentially unchanged. This indicates that the crystal structure remains essentially the same (γ-phase) except iodine atoms are deposited close to specific lattice planes.

Quadratic electro-optic measurements have been performed on the doped films using field-induced birefringence method at 633 nm and 1550 nm. A modulation depth of 0.15% has been observed at 1550 nm for an applied field of 1.15 V/μm for a 0.35μm thick film. The modulation depth had a quadratic dependence on applied field. The Kerr coefficients as measured 3.5x10-10 m/V^2 at 633nm and 2.5x10-10 m/V^2 at 1550nm are exceptionally large and

have been attributed to the subnanometer size metallic domains (quantum dots) formed upon doping and charge-transfer.

Rechargeable batteries have been constructed with sodium chloride (NaCl) dissolved in water with polyvinyl alcohol as additive used as electrolyte, along with two electrodes: 1) stainless steel strip and 2) nonconjugated conductive polymer, iodine doped cis-polyisoprene (natural rubber). The batteries have been characterized measuring currents and voltages with many cycles of charging and discharging. A voltage of 1.5 volts and a maximum current of have been measured. Discharge rate of current has been recorded at definite intervals of time. Polyvinyl alcohol (PVA) added in electrolyte solution at 10-50 % weight of NaCl. A slow down in discharge rate or significant increase in capacity has been observed with increase in concentration of PVA in the electrolyte solution.

Thermal properties of the nonconjugated polymer trans-1,4-polyisoprene have been studied before and after doping with iodine using a differential scanning calorimeter (DSC) over the temperature range of -50 ◦C to 110◦C. The Tm of undoped trans-1,4-polyisoprene has been found to be at 60 ◦C. After doping the T_m transition was not clearly observable.

Optical absorption and refractive index have been studied for heavily doped trans-1,4-polyisoprene. Strong absorption coefficient has seen, larger than 2×10^5 cm^{-1}. Absorption data have used to calculate refractive indices of trans-polyisoprene by Kramers-Kronig Transformation.

BIBLIOGRAPHY

1. M. Thakur, "A class of conducting polymers having nonconjugated backbones" *Macromolecules*, *21* (3), pp 661–664, 1988.

2. M. Thakur, R. Swamy. and J. Titus, "Quadratic Electrooptic Effect in a Nonconjugated Conductive Polymer" *Macromolecules*, *37* (8), pp 2677–2678, 2004.

3. D.V.G.L.N. Roa, P.Wu, B.R. Kimball, M. Nakashima, B.S. Decristofano, "Trends in Optics and Photonics", 63, WB4/1- WB4/3, 2001.

4. M. Thakur, "Nonconjugated conductive polymers" *J. Macromol. Sci., Pure Appl. Chem*., A38 1337, 2001

5. P.N. Prasad, D.J. Williams, "Introduction of Nonlinear Optical effect in molecules and Polymers", *John Wiley &Sons, Newyork,* 1991

6. R. Swamy, H. Rajagopalan, P. Vippa, M. Thakur, A. Sen, "Quadratic electro-optic effect in a nano-optical material based on the nonconjugated conductive polymer, poly(ethylenepyrrolediyl) derivative", *Solid State Communications* 143, pp 519–521, 2007

7. Jerry I. Dadap, Jie Shan, and Tony F. Heinz, "Theory of optical second-harmonic generation from a sphere of centrosymmetric material: small-particle limit", *JOSA B,* Vol. 21, Issue 7, pp. 1328-1347, 2004

8. Y. R. Shen., "The Principles of Nonlinear Optics", *John Wiley and Sons, Newyork*, 1984.

9. G. P. Agrawal and R. W. Boyd. Contemporary Nonlinear Optics", *Academic Press*, 1992.

10. R. W. Boyd. Nonlinear Optics. *Academic Press*, 2003.

11. Guo-Qing Yu and M. Thakur, "Electrical Conduction in Nonconjugated polymer doped with $SnCl_4$ and $SbCl_5$", *Journal of polymer science: Part B*, Vol. 32, 2099-2104, (1994)

12. M.Thakur, “A Class of Conducting Polymer Having nonconjugated Backbones”, *Macromolecules*, 21, 661-664, 1988

13. Hideki Shirakawa, Edwin J. Louis, et. Al, “Synthesis of Electrically conductive oganic Polymers: Halogens Derivatives of Polyacetylene,$(CH)_X$” *J.S.C Chem. Comm.*, 578 – 580, 1977

14. Jerry I. Dadap, Jie Shan, and Tony F. Heinz, “Theory of optical second-harmonic generation from a sphere of centrosymmetric material: small-particle limit”, *JOSA B*, Vol. 21, Issue 7, pp. 1328-1347, 2004

15. D. A. Kleinman, “Nonlinear dielectric polarization in optical media”, Phys. Rev. 126 (6), 1977 (1962)….. susceptibity

16. Y L. Fletcher, M.A., F.R.S London, “The Optical Indicatrix and the Transmission of Light in Crystals*”, Henry Fkowde, Oxford University Press Ware house, Amen Corner,* 1892.

17. E.G. LOVERING, D.C. WOODEN, “Equilibrium Melting Points of the Low-Melting and High-Melting Crystalline Forms of Trans- 1,4-Polyisoprene”, *J Polym Sci*. (A-2) 9,175-179, 1971

18. C.W. BUNN, “ Molecular Structure and Rubber-like Elasticity, I. The Crystal Structures of Beta Gutta-Percha, Rubber and Polychloro- prene”, *Proc Roy Soc.* A180, 40-66, 1942.

19. DOROTHY FISHER, “ Crystal Structures of Gutta-Percha”, *ProcPhysSoc*. 66:7-16,1953.

20. Konstantin Lukin*,* “Bragg's Law and Diffraction: How waves reveal the atomic structure of crystals” *Mineral Physics Institute SUNY Stony Brook*

21. Bragg reflection -- Encyclopedia Britannica: *http://www.britannica.com/EBchecked/topic/76973/Bragg-law*

22. Hillar M. Rootare, “Determination of Phase Transitions in Gutta-Percha by Differential Thermal analysis”, *J DENT RES* 1977; 56; 1453

23. Bragg WH (1912). "On the direct or indirect nature of the ionization by X-rays". Phil. Mag. 23: 647.

24. Friedrich W, Knipping P, von Laue M (1912). "Interferenz-Erscheinungen bei Röntgenstrahlen". Sitzungsberichte der Mathematisch-Physikalischen Classe der Königlich-Bayerischen Akademie der Wissenschaften zu München , 1912

25. Bragg WL, "The Specular Reflexion of X-rays". Nature 90: 410, 1912

26. Bragg WL, "The Diffraction of Short Electromagnetic Waves by a Crystal". *Proceedings of the Cambridge Philosophical Society* **17**: 43, 1913

27. Bragg, "Die Reflexion der Röntgenstrahlen", *Jahrbuch der Radioaktivität und Elektronik* 11: 350, 1914

28. Bragg, "The Structure of Some Crystals as Indicated by their Diffraction of X-rays". *Proc. R. Soc. Lond,* A89 (610): 248, 1913

29. Bragg WL, James RW, Bosanquet CH, "The Intensity of Reflexion of X-rays by Rock-Salt", *Phil. Mag*. 41: 309, 1921

30. Leonid V. Azaroff " Element of Xrayc crystallography, *McGrawHill Inc.*

31. R. J. D. Tilley, "Understanding solids: the science of materials"

32. J.W Jeffery, "Method in X-ray crystallography", *Academic Press London and new york* (1917)

33. J. E. Nickels, M. A. Fineman, W. E. Wallace, "X-Ray Diffraction Studies of Sodium Chloride–Sodium Bromide Solid Solutions", *J. Phys. Chem*., 53 (5), 625–628, 1949

34. SII Nanotechnology, "Specific Heat Capacity Measurement Using DSC-I" *Japan* (1981)

35. Bu-Xuan Wang, Le-Ping Zhou, Xiao-Feng Peng, "Surface and Size Effects on the Specific HeatCapacity of Nanoparticles" *International Journal of Thermophysics*, Vol. 27, No. 1, 139-151, (2006)

36. J. Rupp, R. Birringer, " Enhanced Specific Heat Capacity (C_p) measurements (150-300K) of nanometer-sized crystalline materials", *Physical Review B* Vol. 36, 1987

37. R. S. Prasher and P. E. Phelan, *Int. J. Heat Mass Transfer* 42:1991, 1999.

38. Edward G. Lovering, David C. Wooden, "Equilibrium Melting points of the Low melting and High melting Crystalline Forms of trans-1,4-polyisoprene " *Journal of Polymer Science Part A*-2, Vol.9, 175-179, 1971

39. C.K.L. DAVIES, ONG ENG LONG, "Kinetics of crystallization of trans- 1, 4-polyisoprene crystallized in thin films", *Journal of Materials Science*, 14, 2529—2536, 1979

40. Huafeng Shao, Baochen Huang, Wei Yao, Haixia Li, "Synthesis and characterization of low relative molecular weight trans-1,4-poly(isoprene)" *Journal of Applied Polymer Science*, Vol. 107, Issue 6, pages 3734–3738, 2008

41. Yoshiaki Kinemuchi, Ma Sashi Mikami, Keizo Kobayashi, Koji Wateri, and Yuji Hotta, "Thermoelectric Properties of Nano grained ZnO", *Journal of Electronic Materials*, Vol. 39, No. 9, 2010

42. Li Jiangtian, Guo Limin, Lingxia Zhang, Chichao Yu, " Donor–p–acceptor structure between Ag nanoparticles and azobenzene chromophore and its enhanced third-order optical non-linearity", *Dalton Trans*., 823–831, 2009

43. Hideyuki Inouye, Koichiro Tanaka, Ichiro Tanahashi, "Mechanics of a Terahertz Optical Kerr Shutter with a Gold Nanoparticle System", *Journal of the physics Society of Japan,* Vol. 68 pp3810-3812, 1999,

44. A. Cetin , R. Kibar , M. Hatipoglu , Y. Karabulut , N. Can. "Third-order optical nonlinearities of Cu and Tb nanoparticles in SrTiO3", *Physica B* 405, 2323–2325, 2010

45. Silvina Cerveny, Philippe Zinck, Michael Terrier, Silvia Arrese-Igor, Angel Alegriaand Juan Colmenero. "Dynamics of Amorphous and Semicrystalline 1,4-trans-Poly(isoprene) by Dielectric Spectroscopy", *Macromolecules, vol.* 41,8669-8676, 2008

46. Seong-Min Ma1, JaeTae Seo1, WanJoong Kim "Cubic Nonlinear Optical Properties of Ag Nanoparticles and Ag/Au Coreshells", *Journal of Physics: Conference Series* 109 (2008).

47. Hideyuki Inaiye, Koichiro Tanaka "Femtosecond optical Kerr effect in Gold Nanopartical system", *Jpn. J. Appl. Phys*. Vol-37, L1520-1522, 1988

48. Y. Lin, J. Zhang, E. Kumacheva, "Third-order optical nonlinearity and figure of merit of CdS nanocrystals chemically stabilized in spin-processable polymeric films" *Journal of Material Science* 39, 993– 996, 2004

49. H. H. Huang, F. Q. Yan, Y. M. Kek "Synthesis, Characterization, and Nonlinear Optical Properties of Copper Nanoparticles" *Langmuir*, 13, 172-175, 1997

50. R. del Coso, J. Requejo-Isidro, J. Solis "Third order nonlinear optical susceptibility of Cu:Al2O3 nanocomposites: From spherical nanoparticles to the percolation threshold" *J. of Appl. Phys*. Vol. 95, No. 5, 2004

51. D. Mohantaa, S. Biswas, and A. Choudhury, "Strong Kerr-signals from optically isotropic ZnSe nanocrystals: a study using Mach-Zehnder principles" *Eur. Phys. J. D* 55, 679–683, 2009

52. Li, W. R.; Xie, X. B.; Shi, Q. S.;, Zeng, H. Y.;, Ou-Yang, Y. S.; Chen, Y. B. *Appl Microbiol Biotechnol*, *85(4),* 1115-22, 2010

53. Lubick, N. Environ. *Sci. Technol*., *42 (23),* 8617, 2008

54. Jirakorn ThisayuktaY, Hiroyuki Shiraki, Yoshio Sakai, Takenori Masumi, Sudarshan Kundu, Yukihide Shiraishi, Naoki Toshima and Shunsuke Kobayashi,"Dielectric Properties of Frequency Modulation Twisted Nematic LCDs Doped with Silver Nanoparticles", *Japanese Journal of applied physics*, Vol. 43, 5430-5434, 2004

55. Stephan Link and Mostafa A. El-Sayed, "Size and Temperature Dependence of the Plasmon Absorption of Colloidal Gold Nanoparticles" *J. Phys. Chem. B, 103,* 4212-4217, 1999

56. R.H. Magruder III, Li Yang and R.F. Haglund Jr, "Optical properties of gold nanocluster composite formed by deep ion implantation in silica", *Appl. Phys. Lett.* 62(15), 1730-1732, 1993

57. Survey of Rechargeable Battery Technology, Report to Lawrence Livermore National Laboratories, *Arthur D. Little, Inc*. July 2003

58. T.R. Crompton, " Battery Reference Book", *Butterworth Heinmann* Ltd 1995

59. Techanical Marketing Staff of Gates Energy Products Inc., "Rechargeable Batteries Application Handbook", *Butterworth Heinmann*, Ltd. 1992

60. Robert W. Graham, " Rechargeable Batteries Advance Since 1977" *Noyes Data Corporation*, 1980

61. SBI Energy report, "Advanced Storage Battery Market: from Hybrid/Electric Vehicles to Cell Phones", March 2009.

62. Eric Seale, "Batteries compared ", 2003: *http://www.solarbotics.net/library/pieces/parts_elect_pass_batcomp.html*

63. N. Vasanthan and A. E. Tonelli, "FTIR investigation of the inclusion compound formed between trans-I ,4-polyisoprene and urea", *Polymer,* Vol. 36 No. 25, pp. 4887-4889, 1995.

64. Arthur E. Wooward, N. Vasanthan, and Joseph P. Corrigan, "Infra red spectroscopic investigation of bulk crystallized trans-1,4-polyisoprene", *Polymer,* Vol.34 No.11, 1993

65. D. A. Kleinman, "Nonlinear dielectric polarization in optical media", *Phys. Rev*. 126 (6), 1977, 1962

66. V. Arjunan a, S. Subramanian a, S. Mohan "Fourier transform infrared and Raman spectral analysis of trans-1,4-polyisoprene" *Spectrochimica Acta Part A* 57, 2547–2554, 2001

67. R. de Kronig , "On the theory of the dispersion of X-ray", *J.Opt. Soc. Am*. 12(6), 547, 1926

68. D.C. Hutchings et al., " Kramers-Kronig in nonlinear optics", *Opt. Quantum Electron*. 24, 1, 1992

69. Joseph Habib Simmons, Kelly S. Potter, " Optical materials" 2000

70. V. Deiogio, Christos Flytzanis, " Nonlinear optical Materials: Principle and Applications" , Varenna on Lake Como, 1993

71. H. Bach & N. Neuroth (Editors), "The properties of optical glass", Springer Verlag 1998

72. Rudlger Paschotta , "Encyclopedia of Laser Physics and Technology" *http://www.rp-photonics.com/refractive_index.html*

73. P. S. Kalsi, "Spectroscopy of Organic Compounds" New Age International, 2007

74. George Socrates, "Infrared and Raman characteristic group frequencies: tables and charts", *John Wiley and Sons*, 2004

75. P. Vippa, H. Rajagopalan, M. Thakur, "Electrical and Optical Properties of a Novel Nonconjugated Conductive Polymer, Poly(b-pinene)", *J Polym. Sci. Part B: Polym. Phys*. 43: 3695–3698, 2005

76. Yuan Yang, Matthew T. McDowell, Ariel Jackson, Judy J. Cha, Seung Sae Hong, and Yi Cui, "New Nanostructured Li2S/Silicon Rechargeable Battery with High Specific Energy", *American Chemical Society: Nano lett*. 2010

77. Veeraraghavan Ramamurthy, "Rechargeable Batteries Based On Specific Nonconjugated Conductive Polymers; Electrical, Optical And Structural Studies" *Thesis, Auburn University*, 2007

78. A. Narayanan and M. Thakur, *Solid State Comm*., 150, 375, 2010

79. S. L. Hsu, A. J. Signorelli, G. P. Pez, and R. H. Baughman, *J. Chem. Phys*., 69,1978 106.

80. Richard B. M. Schasfoort, Anna J. Tudos , "Handbook of surface plasmon resonance", *Royal Society of Chemistry*, 2008

81. Dean, John A., "The Analytical Chemistry Handbook", *New York: McGraw Hill*, 1995

82. S. Shrivastava and M. Thakur, Solid State Comm., 151, 775, 2011